Energy efficiency of fiber versus microwave, mmWave, copper, satellite and laser for the transport of the fronthaul and backhaul in 4G and 5G mobile networks
Full Deliverable

IoT Lab

December 2021

Contents

Acronyms

3GPP Third Generation Partnership Project. 2, 3, 9, 57

BBU Base Band Unit. 5, 11, 12, 17, 19, 21, 24, 26

CAPEX Capital Expenditure. 4

COGW Central Office Gateway. 5, 12, 15, 17–19, 21, 25–27, 29

CSGW Cell Site Gateway. 5, 12, 17, 25

DSL Digital Subscriber Link. 16

ETSI European Telecommunications Standards Institute. 2, 3, 9, 57

FSO Free Space Optics. 2, 7, 8, 57

FSO/RF Free Space Optics/Radio Frequency. 8

GES Gigabit Ethernet Switch. 7, 22

Het-Net Heterogeneous Network. 9

LEO Low Earth Orbit. 7

LOS Line of Sight. 8

MIMO Multiple-Input Multiple-Output. 1, 32, 41, 43

mMTC massive Machine Type Communications. 1, 10

mmWave millimeter wave. 1, 2, 6, 15, 19, 21–23, 26–28

NAP Network Access Point. 1, 3, 11, 17, 24

NOMA Non Orthogonal Multiple Access. 1

OAN Optical Aggregation Node. 6, 12, 15, 17, 21, 25–27

OFDMA Orthogonal Frequency Division Multiple Access. 1

ONU Optical Network Unit. 6, 15, 21, 26

OPEX Operating Expenditure. 4

P2P point-to-point. 6, 12, 13, 15, 18, 20–22, 27

RAN Radio Access Network. 1

RRH Remote Radio Head. 6, 11, 17, 20, 24, 26

SISO Single-Input Single-Output. 32

SNR Signal to Noise Ratio. 1, 8

Sub-6GHz . 1, 2, 6, 10, 12, 17, 32, 41

TCO Total Cost of Ownership. 1

URLLC Ultra Reliable Low Latency Communications. 1, 10

vCORE Virtual Stand-Alone Core. 6, 19, 21, 22

vDU/vCU Virtual Distributed Unit and Virtual Centralized Unit. 6, 19–21

Abstract

This technical report has been developed by IoT Lab of Politecnico di Milano in the context of the study "Energy efficiency of fiber versus Microwave, mmW, Copper, Satellite, Laser for the transport of the fronthaul/backhaul in 4G and 5G mobile networks", requested by Prysmian Group and Europacable. The aim of the study is to investigate the energy consumption of the several technologies that are adopted in modern cellular communication (i.e. from 4G onwards) to provide connectivity to the Network Access Point (NAP) and understand which one provides the best performance along this dimension. The topic has been investigated in the specific literature, however, a comprehensive model that harmonize the literature evidence based on actual field data is necessary to comprehend the results and illustrate the limitations of the different technologies. Hence, the study provides a mathematical simulative model[1] that interpolates the field data and estimates the consumption in different scenarios. In accordance with the main literature findings and the field data recovered, we show that optical fiber is the optimal technology for both backhaul and fronthaul in all the scenarios and architectures considered. In fact,both 4G and 5G, with gains between 2-45% (5G Sub-6GHz), 13-54% (5G mmWave) and 20-63% (4G) compared to radio link technology, while in comparison to copper fiber reduces power consumption of a term between 32-54% (4G), 16-22% (5G) and 13-29% (5G mmWave), depending on the scenario.

[1]The model is attached to the study as MATLAB code, while the input data processed that provide the results are reported in Excel sheets.

Chapter 1

Introduction

The tremendous growth of the traffic demand generated by mobile devices (e.g. smartphones and tablets) in 4G networks and the upcoming rise of massive Machine Type Communications (mMTC) and Ultra Reliable Low Latency Communications (URLLC) use cases envisioned by 5G require several optimizations and radical changes to existing infrastructure. Advanced technologies have been developed to fulfil the need of bandwidth and reduce latency: Orthogonal Frequency Division Multiple Access (OFDMA), Multiple-Input Multiple-Output (MIMO) transmission/reception and cell densification form the basis for 4G standards like LTE and LTE-advanced Radio Access Network (RAN). Moreover, several other improvements are under investigation and will play a key role in future 5G and beyond networks, including the adoption of mmWave communications, beamforming and Non Orthogonal Multiple Access (NOMA).

The implementation of such technologies has severe implications over the energy consumption of the whole network, as they require both an increase of computational power to run the algorithms in the base stations and changes in the physical network deployment. For instance, mmWave are characterized by a weak penetration power and lower range (at fixed antenna gains) compared to Sub-6GHz, which prevents them to be used at far distances or in presence of obstacles (even as thin as umbrella foil). To cope with this issue, beamforming techniques allow to concentrate the radiated power in specific directions, pointing towards the receiver and increasing the overall channel Signal to Noise Ratio (SNR). However, this may not be sufficient, and network densification becomes mandatory.

With the introduction of 5G, it has been estimated in [1] that the average cell site power for a macrocell that supports 5G connectivity will increase of 68% compared to a cell supporting 4G and the previous technologies. To prevent the Total Cost of Ownership (TCO) from exploding, it becomes crucial for the network operator to understand which are the technological options for the network deployments and how do they impact on the overall energy consumption in 4G and 5G scenarios.

IoT Lab, interdepartmental laboratory of Politecnico di Milano, has been in-

volved with the aim of analyzing the several backhaul and fronthaul technologies and find out which are the most performative in terms of energy consumption.

1.1 Application context

It is crucial for a mobile operator to understand the impact of specific technological and architectural upgrades in the mobile back- and fronthaul networks on the capital and operational expenditure (i.e., CAPEX and OPEX), in both greenfield and brownfield scenarios. To address this topic, the study considers both 4G and 5G networks with all the possible options that the technology may offer. These are:

- Optical fiber;
- Radio Link;
- Copper;
- Satellite;
- Free Space Optics (FSO);

The study includes both microwave and mmWave, as the two branches of the radio spectrum are widely used in all the cellular scenarios, and especially those envisioned in 5G. Moreover, we consider satellite and FSO among the other technologies, as they have attracted interest in some specific use cases, such as providing connectivity in areas unreachable by terrestrial networks.

1.2 Evaluation methodology

The study has been developed in 5 phases:

1. Literature review;
2. Model definition;
3. Data collection;
4. Data processing;
5. Results interpretation.

In particular, the literature review includes the most relevant peer-reviewed papers published in the past 10 years, for a total of 32 papers. To account for the cellular network scenario's evolution in time, we have included the Third Generation Partnership Project (3GPP) and European Telecommunications Standards Institute (ETSI) recommendations on the technologies, the architectures and the applications. Following the work presented in the literature, we build

a mathematical model that covers the reference architectures, and their implementation in real-world applications. The model is fed with energy consumption data that were collected developing the research, which can be aggregated in 3 clusters:

- Network data: energy consumption of a whole network architecture (e.g., related to an urban area);
- Cell data: energy consumption of a cellular NAP (i.e., macrocell, microcell, pico and femtocell);
- Device data: energy consumption of single devices used in point-to-point links (e.g., optical routers, Ethernet switches, radio transmitters and receivers).

In order to complete the model used for our simulations we collected additional information on the networks such as:

- Environment data: information on the distribution of buildings for femtocells scenarios (e.g., building density) and data on user traffic demand;
- Radio access network data: technologies used for the radio access network (e.g., bandwidth, frequencies, antennas);

The model interpolates the field data and produces the power consumption curves that allow for the comparison between the architectures in the different scenarios. After the curves have been produced, these are interpreted and discussed, underlining the differences between technologies used in both fronthaul and backhaul and conclude the analysis.

1.3 Report structure

The report structure is summarized as follows:

Chapter 2 introduces the technologies adopted in 4G and 5G networks for mobile fronthauling and backhauling. After a discussion on the main technological aspects, the classes of devices included in the energy model are presented.

Chapter 3 introduces the energy model for the cellular networks. We recall the 4G and 5G scenarios definition from the 3GPP and ETSI and then we define the reference network architectures that will be considered later for the evaluation benchmark of the given technologies.

Chapter 4 reports the network, cell and device energy consumption data included in our model. Environment data such as extension, population and building density of Urban, Sub-urban and Rural areas are reported here as well. The results have been validated by comparison to the network data, whenever available.

Chapter 5 presents the numerical results obtained by feeding the model with the data collected in the previous chapter.

Chapter 6 summarizes the work and provides the conclusions.

Chapter 2

Technology overview

In this chapter, we review the technologies dedicated to the transmission of information in cellular networks fronthaul and backhaul, answering the following questions:

- Is the technology used in fronthaul and/or backhaul?
- Which use cases can the technology support?
- Which are the pros and cons of each technology?

This will help in reducing the problem by considering how technologies are applied in real-world use cases, simplifying the design of the energy model. Then, we describe the devices and technological standards that we include in the energy consumption model.

2.1 Optical fiber

Optical fiber is the core technology in modern cellular network for both fronthaul and backhaul. Due to its low cost of production, large bandwidth, low power per transmitted bit and attenuation per kilometer, it represents the enabling technology for both present and future generation of cellular networks. Moreover, as the technology develops towards multi-mode fiber and complex modulation schemes, the capacity of optical fiber is expected to increase even more in the next years.

From the OPEX perspective, one major advantage with respect to radio technology is that it has no spectrum licenses limitations, which is one of the higher costs that operators incur when planning the spectrum bandwidth. On the other hand, the main disadvantage of the technology is the infrastructural deployment investment, which increases with network capillarity. A detailed analysis of the OPEX and CAPEX trade-off is presented in [2] and [3].

This study considers optical transmission devices that support the following hardware interfaces:

- **SFP** (small form factor pluggable) is a compact, hot-swappable transceiver designed to support communication standards such as Ethernet 100/1000 Mbps, Fiber Channel and SONET, among others. Transceivers support speeds up to 4.25 Gbps and are commonly used in applications such as telecommunications and data communications. SFP ports are found in various devices, from Ethernet switches to routers, from network interface cards to firewalls. The small form factor pluggable specification is based on IEEE802.3 and SFF-8472;

- **SPF+**: with transceivers approximately identical in size and appearance, the main difference is that SFP+ is an upgraded version that supports higher speeds of up to 10 Gbps. The difference in data rates also results in a difference in transmission distance, as SFP is generally characterized by a longer transmission distance. SFP+ specifications are based on SFF-8431. In terms of compatibility between SFP and SFP+, SFP+ ports often accept SFP optical fibers but at a reduced speed of 1 Gbps, while it is not possible to connect an SFP + transceiver to an SFP port as SFP+ does not support speeds below 1 Gbps.

- **QSFP** (quad small form factor pluggable) is another type of compact, hot-swappable transceiver. It supports Ethernet, Fiber Channel, InfiniBand and SONET/SDH standards with different data rate options. QSFP modules are commonly available in different types: 4x 1 Gbps QSFP, 4x 10 Gbps QSFP+, 4x 28 Gbps QSFP28.

- **QSFP+** and **QSFP28** are the latest versions, supporting numerous 40 Gbps and 100 Gbps applications. Both QSFP+ and QSFP28 modules integrate 4 transmission channels and 4 reception channels. While QSFP+ supports 4x 10Gbps or 1x 40 Gbps, QSFP28 can do 4x 25 Gbps, 2x 50 Gbps or 1x 100 Gbps, depending on the transceiver used. QSFP specifications are based on SFF-8436.

To estimate the power consumption of the devices belonging to these technologies, we included in the database the values available both in commercial catalogs such as [4] and [5] as well as those presented by the authors in the literature, indicating the primary information source as a reference when citing other authors. We do not consider devices that are used in the backbone network architecture, as the energy consumption analysis in this scenario is out of work's scope.

The devices are grouped into 6 families, according to their function and placement in the network:

- Cell Site Gateway (CSGW): devices that supports Layer-2, Layer-3 functions which provide connectivity to macrocell or microcell Base Band Unit (BBU) via the optical connections listed above;

- Central Office Gateway (COGW): devices that are directly connected to the backbone core network and provide connectivity to aggregation nodes;

- Virtual Stand-Alone Core (vCORE): devices that are directly connected to the backbone core network and implement all 5G Core functions using virtualization;
- Virtual Distributed Unit and Virtual Centralized Unit (vDU/vCU): devices that are connected to the Virtual Stand-Alone Core (vCORE) and run all the 5G virtualized network functions needed to provide connectivity to Remote Radio Head (RRH) ;
- Optical Aggregation Node (OAN): such as the WDM transponders in [4].
- Optical Network Unit (ONU): small devices such as consumer's router or switches.

2.2 Radio Link

This section presents the radio link devices included in the analysis. We distinguish between Sub-6GHz and mmWave in order to clarify which scenario each technology applies to.

2.2.1 Microwave

Microwave frequency bands have been adopted in radio link backhauling since the very beginning with differences among countries according to the national indications. These kind of frequencies are used when the area to be served is so big that other technologies such as mmWave cannot cover it adequately and when it is needed to keep the costs down.

2.2.2 mmWave

mmWave have always attracted the interest of both academy and the industry due to the high bandwidth availability at such high frequencies. However, this come at the price of higher attenuation and low penetration power, which is the main reason why before 5G these have been used mostly for radio bridges, where cable solutions were impracticable and too expensive. One of the limiting factors in the use of mmWave is the design cost of the electronic circuitry and components to handle such high frequencies, which is due to several technical challenges that this kind of electronics has to face when deployed in action. In our model, mmWave are used for the radio backhaul in the 5G scenario. In particular we adopted point-to-point mmWave links at frequency between 71 and 76 GHz, that guarantee a throughput of 10 Gbps [6].

2.2.3 Applications

In the 4G scenarios, for radio link backhauling we considered only Sub-6GHz frequencies, while for 5G we used mmWave by means of P2P links, with differ-

ences between macro- micro- and femtocells. A more useful distinction between the cell architectures will be formally addressed in 3.2 and 3.3.

2.3 Copper

Copper was the dominant cabling technology before the development of the optical fiber technology. It is still widely used for backbone infrastructure cabling, and it is at the foundation of technologies such as Ethernet and ADSL, especially for the last-mile connections towards the homes. The major issue of copper is the lower bandwidth compared to optical fiber and microwaves, which often prevents the technology to be adopted in backhauling architectures. However, the study considers copper as an option for fronthauling in 4G networks, regardless of the aforementioned limitations and in order to evaluate its energy consumption impact on the architectures. The copper devices considered in the study are Gigabit Ethernet Switch (GES), which rely on copper cable to connect the end-point devices.

2.4 Other technologies

There are few other technological options considered in our study: satellite for the backhauling infrastructure and FSO for fronthauling. These are rarely used compared to fiber, copper, and microwave to provide network connectivity: because of their physical limitations, they are confined to specific use cases where the other options are not feasible. Moreover, we show that from the energy consumption perspective these are not convenient options for the scenarios and architectures considered.

2.4.1 Satellite

Satellite has been used to provide connectivity in areas where the deployment of an earth infrastructure has been proved to be unfeasible, e.g., because of the high costs with the respect of user coverage and morphological characteristics of the deployment location [7]. Moreover, satellite links have the advantage to provide connectivity in extreme scenarios such as earthquakes, even though mmWave UAV technology is envisioned to be replacing this strategy in 5G scenarios [8]. Modern application of satellite communication for backhauling are envisioned by 3GPP in Release 17, especially exploiting Low Earth Orbit (LEO) satellites. These have been investigated by literature review, with some specific papers addressing the problem [9]. However, no evidence of energy advantage compared to terrestrial infrastructure, nor data on power consumption in satellite communications has been found to support such statement. Generally speaking, the high TCO for constellation and the long microwave communication links are the reason that confine this technology to extreme use cases [9].

2.4.2 Free Space Optics

FSO is a technology that is used for high bandwidth point-to-point links. There are strong physical limitations that restrict the application fields, including:

- Mandatory Line of Sight (LOS): small deviations and obstacles in pointing transmitter and receiver may determine the system failure;
- Diffraction: laser beams suffer from diffraction phenomena, which cause energy to diverge in space instead of focusing at one point;
- Strong weather attenuation: laser beams are heavily attenuated by fog, rain, and atmospheric agents in general, which are usually uncontrolled.

Indeed, these were the main reasons that pushed the research around optical fiber, i.e., developing a solution that could beat diffraction, allow light to bend around obstacles and resist the environment conditions [10]. However, in some 5G scenarios Free Space Optics/Radio Frequency (FSO/RF) have been recently considered as a solution to maintain high dataflows where optical fiber can't be deployed, especially in fronthaul [11]. This is a short link solution, ranging from meters to few kilometers, which relies on switching between laser and radio according to the weather conditions (i.e., the optical link SNR) [12]. However, from an energy consumption perspective it has been shown that FSO the technology demands 10 times more energy to provide the same output power (i.e., the same link performance) compared to optical fiber, even when transmitter and receiver are closed together and diffraction/atmospheric effects are negligible [13]. Moreover, when switching from FSO the RF the comparison reduces to optical fiber versus radio, which sees optical fiber as the winning technology, as shown in the following Chapters.

Chapter 3

Energy model

In this chapter, we introduce the energy model for assessing the network consumption and compare the technologies. The model is structured and implemented as a cascade of 3 blocks, where the output of the previous block feeds the following. In order:

1. **Scenario** sets the combination of cellular technology and the application environment i.e., 4G/5G and Urban, Suburban or Rural for the technology and application environment, respectively. The cellular technology defines which types of cellular cells are considered, with the difference that 5G adds mmWave cells, while the application environments are defined as in the 3GPP and ETSI documentation for 4G and 5G technologies [14].

2. **Architecture** defines the possible architecture applicable in 4G and 5G defined scenarios. We consider Heterogeneous Network (Het-Net) deployments combining the reference architecture presented in [2] for backhauling with the options for fronthauling illustrated in [15], to overcome the limitations of the two models and provide a complete architecture pattern for our analysis. Concretely, the block defines the network topology, the back- and fronthaul technologies and the cell dimension.

3. **Devices** The last block defines the numerical values of device power consumption to be processed to obtain the overall network power consumption, according to the 3 clusters: network, cell and device data.

3.1 Scenarios

According to the 3GPP, there are 12 deployment scenarios to be studied in the deployment of cellular networks [14]. We distinguish between 4G scenarios, i.e., scenarios that were addressed by 4G technology, and 5G scenarios, as a counterpart. According to the 3GPP nomenclature, we integrate in our analysis the following scenarios: Indoor hotspot, Dense urban, Rural and Urban macro,

as they provide the needed variability to assess the energy consumption for the technologies at hand. 5G extends these scenarios with new ones oriented to mMTC and URLLC, such as: Urban coverage for massive connection and Urban Grid for Connected Car.

4G/5G Sub-6GHz Scenarios

Decoupling the application environment from the technology, we obtain Table 3.1 which includes the 3GPP scenarios discussed so far:

Scenario	Macrocell	Microcell	Pico/Femtocell
Urban	Urban macro	Dense Urban	Indoor hotspot
Sub-urban	Sub-urban macro	Dense sub-urban	Indoor hotspot
Rural	Rural macro	Rural micro	Indoor hotspot

Table 3.1: Scenarios versus technology table.

The model parameters that define each application environment, which will be used to compute the network bandwidth demand and provide the network plan in the following chapter, are reported later in Table 4.5.

5G mmWave Scenarios

For the 5G mmWave case we have reconstructed the following environments and architectures:

Scenario	Macrocell	Pico/Femtocell
Urban	Urban streetmacro	Indoor hotspot
Sub-urban	Sub-urban streetmacro	Indoor hotspot
Rural	Rural streetmacro	Indoor hotspot

Table 3.2: Scenarios versus technology table.

The environmental parameters remain the same, except for the microcell scenario since it wasn't considered, and are reported later in Table 4.5.

3.2 4G Network Architectures

The network architecture that supports the identified scenarios is represented in 3.1. As a reference, the Figure pictures the elements considered in the analysis for a optical fiber based back- and fronthaul. When considering different technologies, i.e., microwave for macro- and microcell, and microwave or copper for femtocell, the changes in the architecture will be displayed.

3.2.1 Macrocell

According to [2, 14, 15], we define macrocell as cellular NAP that can provide connectivity up to $C_{\mathrm{M,max}} = 600$ [Mbit/s], while serving approximately 3,000 people. This results in a coverage area up to 1 Km^2 for an Urban environment, while growing for Sub-urban and Rural, extending to tens of Km^2 of coverage. The power consumption of a macrocell can be computer as [15]:

$$P_{\mathrm{M}} = P^{4G}_{\mathrm{BBU,M}} + N_{\mathrm{sec,M}} P^{4G}_{\mathrm{RRH,M}}, \tag{3.1}$$

where $P^{4G}_{\mathrm{BBU,M}}$ indicates the power consumed by the macrocell Base Band Unit (BBU), $N_{\mathrm{sec,M}}$ represents the number of the macrocell sectors and $P^{4G}_{\mathrm{RRH,M}}$ is the Remote Radio Head (RRH) power consumption required to radiate $P^{4G}_{\mathrm{max,M}}$ at each of the $N^{4G}_{\mathrm{ant,M}}$ transmitting antennas per sector. $P^{4G}_{\mathrm{max,M}}$ is the maximum radiated power before reaching the saturation region of the power amplifier, which is required to achieve both full capacity and maximum coverage. The results in [16] and [17] show that the impact of daily load variations on 4G/LTE networks back- and fronthaul power consumption is negligible, however, we will consider both the case where the number of NAP is tailored on the traffic demand (i.e. all cells consume full power to provide coverage and throughput), and the case where given the network deployment the traffic load reduces to zero, bringing the NAP to the idle state. In order to estimate the power consumption when the traffic load reduces, we combine the linear approximation presented in [16] and the shannon theorem for channel capacity, as discussed later.

Once $P^{4G}_{\mathrm{max,M}}$ is fixed, we express the contribution to the network power consumption of the fronthaul interface between BBU and RRH, $P_{\mathrm{FH,M}}$, and split the RRH power consumption between the power amplifier $P_{\mathrm{PA,M}}$ and the RF chains $P_{\mathrm{RF,M}}$. Therefore, equation (3.1) can be rewritten as:

$$P_{\mathrm{M}} = \left(P_{\mathrm{DSP,M}} + P_{\mathrm{FH,M}} + N_{\mathrm{sec,M}} N^{4G}_{\mathrm{ant,M}} \left(P_{\mathrm{PA,M}} + P_{\mathrm{RF,M}}\right)\right) \Delta^{4G}_{\mathrm{loss,M}}, \tag{3.2}$$

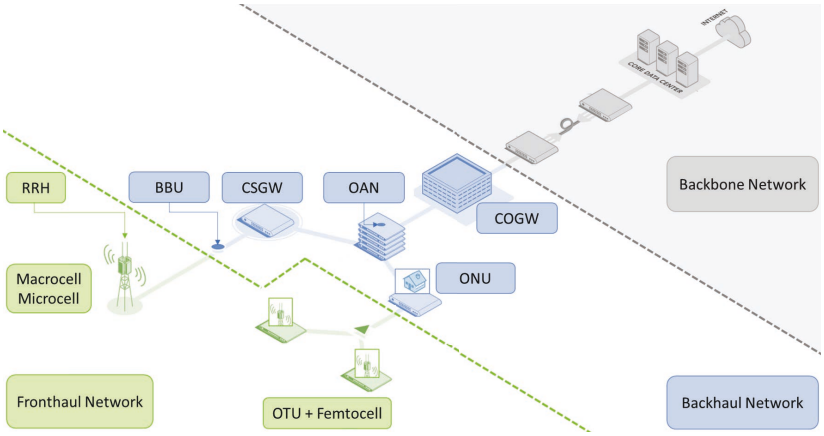

Figure 3.1: Reference architecture overview.

where $P_{\mathrm{DSP,M}} = P^{4G}_{\mathrm{BBU,M}} - P_{\mathrm{FH,M}}$ is the power of the BBU fully dedicated to baseband digital signal processing (DSP). Finally, $\Delta^{4G}_{\mathrm{loss,M}}$ accounts for the cooling plant and the DC power supply losses in site.

Optical fiber backhauling

Schematized in Figure 3.2, the network architecture is such that the BBU is served by a CSGW, which is connected to the backbone network by means of an OAN and a COGW. Every OAN aggregates $N_{\mathrm{SUB}} = 7$ macrocells by connecting them over a standard optical fiber cable, while every COGW aggregates $N_{\mathrm{AGG}} = 60$ OAN. Hence, the overall network consumption is:

$$P_{\mathrm{M,opt}} = N_{\mathrm{M}} \left(P_{\mathrm{M}} + P_{\mathrm{CSGW}} + (1 + N_{\mathrm{SUB}}) P_{\mathrm{OPT}}\right) + N_{\mathrm{OAN,M}} \left(P_{\mathrm{OAN}} + P_{\mathrm{OPT}}\right) + N_{\mathrm{COGW,M,opt}} P_{\mathrm{COGW}}, \tag{3.3}$$

where P_{CSGW}, P_{OAN}, P_{COGW} represent the power consumed by the optical CSGW, the OAN and the COGW, respectively, while P_{OPT} is the power consumed by the optical link, according to the standards in Section 2.1. Finally, N_{M} is the total number of macrocell in the network, computed as a function of the network bandwidth demand per square kilometer τ, which is estimated as in [2]:

$$N_{\mathrm{M}} = \left. \frac{(1 - \eta)\, \tau}{C_{\mathrm{M,max}}} \right|_{\eta = 0}, \tag{3.4}$$

where η indicates the femtocell penetration rate, i.e., the percentage of total bandwidth demand that is served by means of femtocells. Lastly, observe that $N_{\mathrm{OAN,M}} = \lceil N_{\mathrm{M}} / N_{\mathrm{SUB}} \rceil$ is the number of OAN and $N_{\mathrm{COGW,M,opt}} = \lceil N_{\mathrm{OAN,M}} / N_{\mathrm{AGG}} \rceil$ is the number of COGW.

Radio link backhauling

In this case, backhauling is provided by N_{H} Sub-6GHz microwave hubs [2]. We assume that one P2P link is established between each microwave hub and

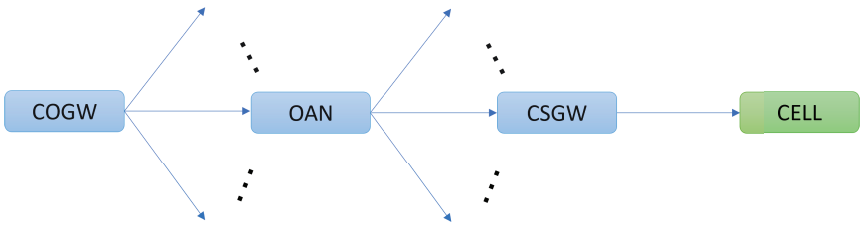

Figure 3.2: Optical fiber backhauling.

$N_{\mathrm{H,L}} = 2$ macrocells of the previous deployment, assuming that the total capacity of the hub is twice the capacity of the macrocell. The hub is composed of two RF chains that feed the P2P links to the macrocells, which contain the same elements as for the macrocell. Thus, the hub power consumption can be computed as:

$$P_{\mathrm{H}} = N_{\mathrm{H,L}} P^{4G}_{\mathrm{RRH,M}} + P^{4G}_{\mathrm{BBU,M}} + P_{\mathrm{CSGW}}, \tag{3.5}$$

while considering the whole network architecture, we have:

$$P_{\mathrm{M,MW}} = N_{\mathrm{M}}(P_{\mathrm{M}} + P^{4G}_{\mathrm{link}}) + N_{\mathrm{H,M}}\,(P_{\mathrm{H}} + P_{\mathrm{OPT}}) + N_{\mathrm{COGW,M,MW}} P_{\mathrm{COGW}}, \tag{3.6}$$

which compared to 3.3 replaces the contributions of the optical connections to the macrocells, CSGW and OAN with the N_{H} microwave links. Moreover, in this case $N_{\mathrm{COGW,M,MW}} = \lceil N_{\mathrm{H,M}}/N_{\mathrm{AGG}} \rceil$ and P^{4G}_{link} accounts for the contribution of the radio link towards the hub.

3.2.2 Microcell

Compared to macrocells, microcells have a lower capacity that we assumed equal to 100 Mbps and omnidirectional antennas [18]. Hence, the power consumption can be computed as:

$$P_{\mathrm{m}} = P^{4G}_{\mathrm{BBU,m}} + P^{4G}_{\mathrm{RRH,m}}, \tag{3.7}$$

where $P^{4G}_{\mathrm{RRH,m}}$ and $P^{4G}_{\mathrm{BBU,m}}$ are the microcell counterparts of the macrocell's RRH and BBU power consumption. This equation can be further expanded as equation (3.2):

$$P_{\mathrm{m}} = \left(P_{\mathrm{DSP,m}} + P_{\mathrm{FH,m}} + N^{4G}_{\mathrm{ant,m}}\,(P_{\mathrm{PA,m}} + P_{\mathrm{RF,m}})\right) \Delta^{4G}_{\mathrm{loss,m}}, \tag{3.8}$$

where $N^{4G}_{\mathrm{ant,m}}$ represents the number of antennas per microcell radiating $P_{\mathrm{max,m}}$ power in order to provide the assumed coverage, while the other terms are the microcell counterparts of the DSP unit, fronthaul connection and RRH terms of the macrocell case. In this case, $\Delta^{4G}_{\mathrm{loss,m}}$ accounts only for the power supply losses, assuming that no cooling system is attached to the microcell.

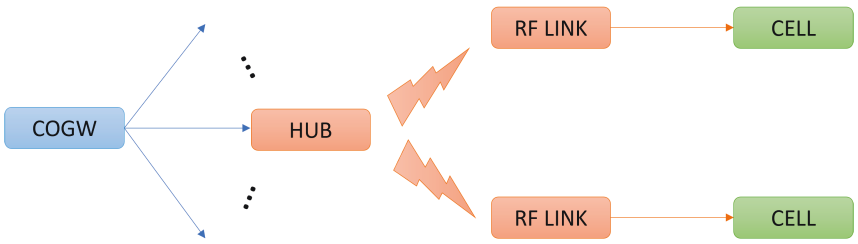

Figure 3.3: Microwave backhauling.

Optical fiber backhauling

Assuming the same topology as the macrocellular scenario, we obtain:

$$P_{\mathrm{m,opt}} = N_{\mathrm{m}} \left(P_{\mathrm{m}} + P_{\mathrm{CSGW}} + P_{\mathrm{OPT}}\right) + N_{\mathrm{OAN,m}} \left(P_{\mathrm{OAN}} + (1 + N_{\mathrm{SUB}})P_{\mathrm{OPT}}\right) + N_{\mathrm{COGW,m,opt}} P_{\mathrm{COGW}}, \tag{3.9}$$

being $N_{\mathrm{OAN,m}}$ the number of OAN and $N_{\mathrm{COGW,m,opt}}$ the number of COGW which are computed in the same way as for macrocells. N_{m} is the total number of microcell in the network, which is assumed to be the maximum between the minimum number of microcells to provide the area coverage, and the number of requested microcells to fulfill the capacity demand:

$$N_{\mathrm{m}} = \max\left(\frac{(1-\eta)\tau}{C_{\mathrm{m,max}}}, \frac{A}{A_{\mathrm{m}}}\right)\Bigg|_{\eta=0}, \tag{3.10}$$

where A is the area of the deployment and A_{m} is the area covered by one microcell.

Radio link backhauling

As previously, we rewrite the equations according to the topology of the macrocell scenario, while assuming $N_{\mathrm{H,L}} = 10$ to account for the lower microcell bandwidth demand. We have:

$$P_{\mathrm{m,MW}} = N_{\mathrm{m}} \left(P_{\mathrm{m}} + P_{\mathrm{link}}^{4G}\right) + N_{\mathrm{H,m}} \left(P_{\mathrm{H}} + P_{\mathrm{OPT}}\right) + N_{\mathrm{COGW,m,MW}} P_{\mathrm{COGW}}, \tag{3.11}$$

which adds to the microcell an additional RRH and antenna to sustain the link towards the microwave hub and $N_{\mathrm{COGW,m,MW}}$ is calculated in the same way as macrocells, that is based on the number of HUBs.

3.2.3 Pico and femtocell

This scenario is characterized by the deployment of small cells inside buildings and apartments, where EM waves do not travel between buildings' floors and walls. Following the modeling steps indicated in [2] which allow to estimate the environment parameters, such as average number of buildings and floors per building, we define three architectures as follows.

Optical fiber fronthauling

As in [2], we assume that connectivity is provided inside the apartments by means of femtocells. The femtocell power consumption is modeled as:

$$P_{\mathrm{f}} = P_{\mathrm{BBU,f}}^{4G} + P_{\mathrm{RRH,f}}^{4G} \tag{3.12}$$

where the indicated powers have the same meaning as for the macrocell and microcell counterparts. This can be further developed as in (3.2) and (3.8), where the terms in the equations have been reported according to the cell size:

$$P_{\mathrm{f}} = \left(P_{\mathrm{DSP,f}} + P_{\mathrm{FH,f}} + N_{\mathrm{ant,f}}\left(P_{\mathrm{PA,f}} + P_{\mathrm{RF,f}}\right)\right)\Delta^{4G}_{\mathrm{loss,f}}. \tag{3.13}$$

With optical fiber fronthauling, shown in Figure 3.1, femtocells are feeded by an ONU that receives an optical fiber from an aggregation node that connects all the units inside the building. Aggregation nodes are grouped by intermediate optical nodes with a capacity of $N_{\mathrm{opt,L}}$ links, and then reaching the access node of the backbone. As a result, the overall network consumption is:

$$\begin{aligned} P_{\mathrm{f,opt}} &= N_{\mathrm{f}}\left(P_{\mathrm{f}} + P_{\mathrm{ONU}} + 2P_{\mathrm{OPT}}\right) + N_{\mathrm{b}}\left(P_{\mathrm{ONU}} + P_{\mathrm{OPT}}\right) \\ &+ N_{\mathrm{OAN,f}}\left(P_{\mathrm{OAN}} + (1 + N_{\mathrm{AGG,f}})P_{\mathrm{OPT}}\right) + N_{\mathrm{COGW,f,opt}}P_{\mathrm{COGW}}, \end{aligned} \tag{3.14}$$

where P_{ONU} represent the power of the ONU, N_{f} and N_{b} are the number of femtocell and buildings, respectively, $N_{\mathrm{COGW,f,opt}}$ is the number of COGW and $N_{\mathrm{OAN,f}} = N_{\mathrm{f}}/N_{\mathrm{AGG,f}}$. In this case each OAN aggregates $N_{\mathrm{AGG,f}} = 72$ cells.

Radio link fronthauling

In this case, we assume that the buildings' roof is equipped with a mmWave P2P antenna, which is connected to an aggregation hub. Femtocells are connected to an Ethernet switch positioned on the roof close to the receiving antenna, while hubs are connected to the backbone as discussed previously. Assuming $N_{\mathrm{H,L,f}} = 8$ as the number of buildings aggregated by an HUB we compute the main terms of the consumption as:

$$P_{\mathrm{ROOFS}} = N_{\mathrm{b}}\left(P_{\mathrm{P2P}} + P_{\mathrm{OPT}}\right), \tag{3.15}$$

$$P_{\mathrm{BUILDINGS}} = N_{\mathrm{b}}\left(2P_{\mathrm{OPT}} + P_{\mathrm{GES}}\right). \tag{3.16}$$

and

$$P_{\mathrm{H,f}} = N_{\mathrm{H,L,f}}\left(P_{\mathrm{P2P}} + P_{\mathrm{OPT}}\right) \tag{3.17}$$

Here N_{b} is the number of buildings which is the same as before and. The overall consumption can be computed as:

$$\begin{aligned} P_{\mathrm{f,MW}} &= N_{\mathrm{f}}\left(P_{\mathrm{f}} + P_{\mathrm{ETH}} + 2P_{\mathrm{CU}}\right) \\ &+ P_{\mathrm{ROOFS}} + P_{\mathrm{BUILDINGS}} + N_{\mathrm{H,f}}P_{\mathrm{H,f}} + N_{\mathrm{COGW,f,MW}}P_{\mathrm{COGW}}, \end{aligned} \tag{3.18}$$

where $N_{\mathrm{H,f}} = \lceil N_{\mathrm{f}}/N_{\mathrm{H,L,f}} \rceil$ is the number of HUBs and
$N_{\mathrm{COGW,f,MW}} = \lceil N_{\mathrm{H,f}}/N_{\mathrm{AGG}} \rceil$ is the number of COGW.

Copper fronthauling

This scenario shares the same topology as the optical fiber scenario, but substitutes the optical infrastructure with copper-based Digital Subscriber Link (DSL) up to the femtocell. The network consumption is obtained as:

$$\begin{aligned} P_{\mathrm{f,CU}} = N_{\mathrm{f}} \left(P_{\mathrm{f}} + 2P_{\mathrm{CU}} + P_{\mathrm{ETH}}\right) + N_{\mathrm{b}} \left(P_{\mathrm{DSL}} + P_{\mathrm{CU}}\right) \\ + N_{\mathrm{OAN}} \left(P_{\mathrm{OAN}} + (1 + N_{\mathrm{AGG,f}}) P_{\mathrm{OPT}}\right) + N_{\mathrm{COGW,f,opt}} P_{\mathrm{COGW}}, \end{aligned} \tag{3.19}$$

where $N_{\mathrm{COGW,f,opt}}$ is the same as in the optical fiber case.

3.2.4 Fixed Architecture Modeling

One of the most insightful analysis that can be done is the one in which a specific network architecture is chosen, which means that the networks are deployed considering a fixed peak traffic. In this case the power needed at the transmitters to satisfy the traffic demand is modeled following the Shannon–Hartley theorem for channel capacity which describes the relationship between channel capacity and the transmitted power via this formula:

$$C = B N_{\mathrm{sec}} N_{\mathrm{ant}} log_2(1 + SNR). \tag{3.20}$$

where C is the channel capacity in Mbps, B is the channel bandwidth in Hertz, N_{sec} is the number of sectors in a given cell, N_{ant} is the number of antennas in a sector and SNR is the signal-to-noise ratio at the receiver. This formula allows for the average transmitted power computation in order to guarantee the selected throughput. The relationship between the transmitted power and the power consumed by the cell is provided in [16], and it is:

$$P_{\mathrm{in}} = N_{\mathrm{sec}} \left(P_0 + \Delta_{\mathrm{p}} P_{\mathrm{out}}\right). \tag{3.21}$$

where (P_0 is the power consumption calculated at the minimum possible output power, Δ_{p} is the slope of the load dependent power consumption and P_{out} denotes the RF output power. This formula holds for all the cell dimensions, as they differ only in the numerical values reported in [16].

3.2.5 Hybrid Urban scenario

In actual urban scenarios, hybrid solutions that mix macrocells, microcells and pico/femtocells are deployed to tailor the cellular coverage on the area at hand [18]. To account for this, we consider two urban scenarios where the macrocells and microcells are deployed beside the femtocells, respectively. The degree of femtocells versus macro- and microcells is determined by the femtocell penetration parameter η, as in [2], ranging between 0 and 1, trivially meaning no femtocells deployed or only femtocell deployed, respectively.

The equations that rule this scenario are the same as the previous scenarios. Hence, the network power consumption in the case of macrocell hybrid scenario is computed as:

$$P_{\mathrm{HYB,M,x}} = P_{\mathrm{M,x}} + P_{\mathrm{f,y}}, \tag{3.22}$$

where x and y define the possible back- and fronthauling technologies. In particular, we consider the (x, y) combinations $(\mathrm{MW}, \mathrm{MW})$, $(\mathrm{MW}, \mathrm{CU})$ and $(\mathrm{opt}, \mathrm{opt})$. The same holds for the microcell:

$$P_{\mathrm{HYB,m,x}} = P_{\mathrm{m,x}} + P_{\mathrm{f,y}}. \tag{3.23}$$

3.3 5G Sub-6GHz Network Architectures

3.3.1 Macrocell

According to [19], we define 5G sub-6 GHz macrocells as cellular NAP that can provide connectivity up to $C^{5G}_{\mathrm{M,max}} = 1800$ [Mbit/s], while we keeping all the assumptions in terms of coverage and served used from the 4G case. The power consumption of a macrocell can be computer as in [15]:

$$P^{5G}_{\mathrm{M}} = P^{5G}_{\mathrm{BBU,M}} + N_{\mathrm{sec,M}} P^{5G}_{\mathrm{RRH,M}}, \tag{3.24}$$

where $P^{5G}_{\mathrm{BBU,M}}$ indicates the power consumed by the macrocell Base Band Unit (BBU), $N_{\mathrm{sec,M}}$ represents the number of the macrocell sectors and $P^{5G}_{\mathrm{RRH,M}}$ is the Remote Radio Head (RRH) power consumption required to radiate $P^{5G}_{\mathrm{max,M}}$ from the $N^{5G}_{\mathrm{ant,M}}$ transmitting antennas per sector. For our simulation we will consider both the case where the number of NAP is tailored on the traffic demand (i.e. all cells consume full power to provide coverage and throughput), and the case where given the network deployment the traffic load reduces to zero, bringing the NAP to the idle state.In order to estimate the power consumption when the traffic load reduces, we combine the linear approximation presented in [20] and the Shannon theorem for channel capacity, as discussed later.

Optical fiber backhauling

Schematized in Figure 3.4, the network architecture is such that the BBU is served by a CSGW, which is connected to the backbone network by means of an OAN and a COGW. Every OAN aggregates $N_{\mathrm{SUB,M}}$ macrocells by connecting them over a standard optical fiber cable, while every COGW aggregates $N_{\mathrm{OAN},M}$. Hence, the overall network consumption is:

$$\begin{aligned} P^{5G}_{\mathrm{M,opt}} = N^{5G}_{\mathrm{M}} \left(P^{5G}_{\mathrm{M}} + P_{\mathrm{CSGW}} + P_{\mathrm{OPT}} \right) \\ + N^{5G}_{\mathrm{OAN,M}} \left(P_{\mathrm{OAN}} + P_{\mathrm{OPT}} N_{\mathrm{SUB}} \right) + N^{5G}_{\mathrm{COGW,M}} P_{\mathrm{COGW}}, \end{aligned} \tag{3.25}$$

where P_{CSGW}, P_{OAN}, P_{COGW} represent the power consumed by the optical CSGW, the OAN and the COGW, respectively, while P_{OPT} is the power consumed by the optical link, according to the standards in 2.1. N^{5G}_{M} is the total

number of macrocell in the network, computed as a function of the network bandwidth demand per square kilometer τ, which is estimated in the same way as previously seen for the 4G scenario with the new capacity:

$$N_{\mathrm{M}}^{5G} = \left.\frac{(1-\eta)\,\tau}{C_{\mathrm{M,max}}}^{5G}\right|_{\eta=0}, \tag{3.26}$$

Lastly, observe that $N_{\mathrm{OAN,M}}^{5G} = \lceil N_{\mathrm{M}}^{5G}/N_{\mathrm{SUB}} \rceil$ and $N_{\mathrm{COGW,M}}^{5G} = \lceil N_{\mathrm{OAN,M}}/N_{\mathrm{AGG}} \rceil$ is the number of COGW.

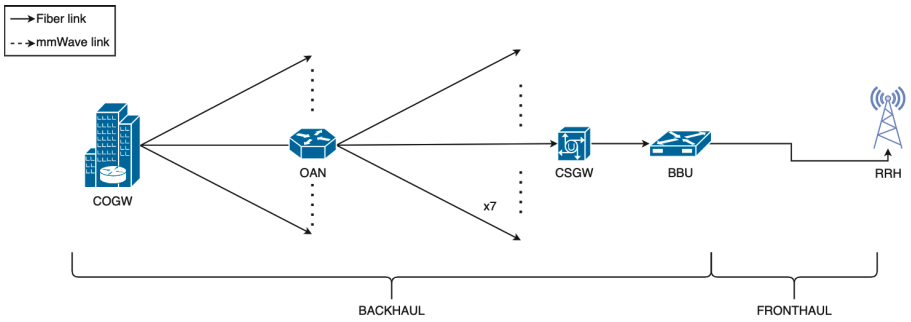

Figure 3.4: Optical fiber backhauling.

Radio link backhauling

In this case, backhauling is provided by N_{H}^{5G} mmWave hubs. We assume that one P2P link is established between a macrocell and a mmWave hub and that each hub aggregates $N_{\mathrm{H,L,M}}^{5G} = 7$ macrocells of the previous deployment. The hub is composed of seven millimeter wave radios that feed the P2P links to the macrocells, which contain the same elements as before plus a millimeter wave radio of the same kind as the ones installed in the hub, as we can see in Figure 3.5. Thus, the hub power consumption can be computed as:

$$P_{\mathrm{H,M}}^{5G} = N_{\mathrm{H,L,M}}^{5G}\left(P_{\mathrm{P2P}} + P_{\mathrm{OPT}}\right) \tag{3.27}$$

where P_{P2P} is the power used by a single millimeter wave radio.Considering the whole network architecture, we have:

$$\begin{aligned} P_{\mathrm{M,MW}}^{5G} &= N_{\mathrm{M}}^{5G}\left(P_{\mathrm{M}}^{5G} + P_{\mathrm{CSGW}} + P_{\mathrm{P2P}} + 2P_{\mathrm{OPT}}\right) \\ &+ N_{\mathrm{OAN,M}}^{5G}\left(P_{\mathrm{OAN}} + P_{\mathrm{OPT}} N_{\mathrm{SUB,M}}\right) + N_{\mathrm{H,M}}^{5G} P_{\mathrm{H,M}}^{5G} + N_{\mathrm{COGW,M}}^{5G} P_{\mathrm{COGW}}, \end{aligned} \tag{3.28}$$

which compared to the previous case include the added contributions of the millimeter wave hubs and radios plus the additional optical ports required. In particular, $N_{\mathrm{H,M}}^{5G}$ is the number of millimeter wave hubs required for the network and is equal to:

$$N_{\mathrm{H,M}}^{5G} = \lceil N_{\mathrm{M}}^{5G}/N_{\mathrm{H,L,M}}^{5G} \rceil; \tag{3.29}$$

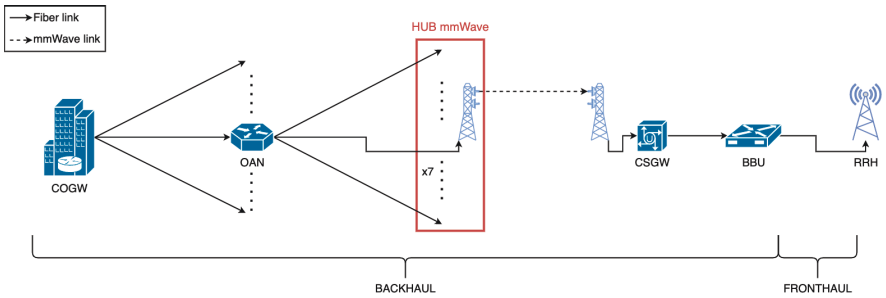

Figure 3.5: mmWave backhauling.

3.3.2 Microcell

Compared to macrocells, microcells have a lower capacity that we assumed equal to 1250 Mbps and omnidirectional antennas [18]. Differently from the 4G case here we implemented a virtualized RAN in which the all the functions of the BBU are replaced by vDU/vCU and vCORE, which also replaces the COGW. Hence, the power consumption of a cell is composed by the radio part only and is equal to $P^{5G}_{\mathrm{RRH,m}}$ which is the microcell counterpart of the macrocell's RRH power consumption while the overall consumption of a cell becomes:

$$P^{5G}_{\mathrm{m}} = P^{5G}_{\mathrm{RRH,m}} + P_{\mathrm{CSGW}} + P_{\mathrm{OPT}}, \tag{3.30}$$

On the other hand , the overall consumption of the vDU/vCU is:

$$P_{\mathrm{vDU/vCU,m}} = N_{\mathrm{vDU/vCU,m}} P_{\mathrm{vDU/vCU}}, \tag{3.31}$$

where $P_{\mathrm{vDU/vCU}}$ represents the power consumption of the Virtual Distributed Unit and Virtual Centralized Unit (vDU/vCU) and $N_{\mathrm{vDU/vCU,m}}$ represents the number of vDU/vCU in the network, which can be calculated knwing that each one supports up to 8 microcells, so:

$$N_{\mathrm{vDU/vCU,m}} = \lceil N^{5G}_{\mathrm{m}}/8 \rceil, \tag{3.32}$$

Finally the overall consumption of the vCORE is:

$$P_{\mathrm{vCORE,m}} = N_{\mathrm{vCORE,m}} P_{\mathrm{vCORE}}, \tag{3.33}$$

where P_{vCORE} is the consumption of a single vCORE and $N_{\mathrm{vCORE,m}}$ is the number of vCORE in the network that can be computed as:

$$N_{\mathrm{vCORE,m}} = \lceil N_{\mathrm{vDU/vCU,m}}/20 \rceil, \tag{3.34}$$

Optical fiber fronthauling

By combining the equations presented in the previous sections following the architecture shown in Figure:3.6 we obtain the following result:

$$P^{5G}_{\mathrm{m,opt}} = N^{5G}_{\mathrm{m}} P^{5G}_{\mathrm{m}} + P_{\mathrm{vDU/vCU,m}} + P_{\mathrm{vCORE,m}} \tag{3.35}$$

N_{m}^{5G} is the total number of microcell in the network, which is calculated in the same way as before, so as the maximum between the minimum number of microcells to provide the area coverage, and the number of requested microcells to fulfill the capacity demand.

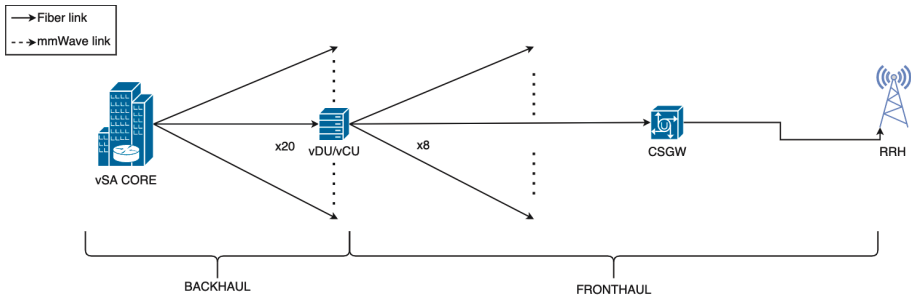

Figure 3.6: Optical fiber fronthauling.

Radio link fronthauling

As seen in the macrocell scenario we implemented the radio connections by means of millimeter wave P2P links as seen before, but since in this case the topology is different, as can be seen in Figure 3.7, they are used in the fronthaul, between the vDU/vCU and the RRH. Moreover in order to be consistent with the number of supported cells in the vDU/vCU we imposed $N_{\mathrm{H,L,m}}^{5G} = 8$, so that each hub serves 8 microcells.

The hub power consumption can be computed as:

$$P_{\mathrm{H,m}}^{5G} = N_{\mathrm{H,L,m}}^{5G} \left(P_{\mathrm{P2P}} + P_{\mathrm{OPT}}\right) \tag{3.36}$$

Then the overall power consumption becomes:

$$P_{\mathrm{m,MW}}^{5G} = N_{\mathrm{m}}^{5G} \left(P_{\mathrm{m}}^{5G} + P_{\mathrm{P2P}} + P_{\mathrm{OPT}}\right) + N_{\mathrm{H,m}} P_{\mathrm{H,m}}^{5G} + P_{\mathrm{vDU/vCU,m}} + P_{\mathrm{vCORE,m}}, \tag{3.37}$$

where, compared to the optical fiber scenario, we have two additional terms that account for the radio systems. In this case the number of hubs is equal to:

$$N_{\mathrm{H,m}}^{5G} = \lceil N_{\mathrm{m}}^{5G} / N_{\mathrm{H,L,m}}^{5G} \rceil; \tag{3.38}$$

3.3.3 Femtocell

As said for 4G, in scenario we deploy small cells inside apartments, where EM waves have difficulties in penetrating. As with microcells we use cells that have a capacity of 1250 Mbps and a virtualized RAN network architecture in which

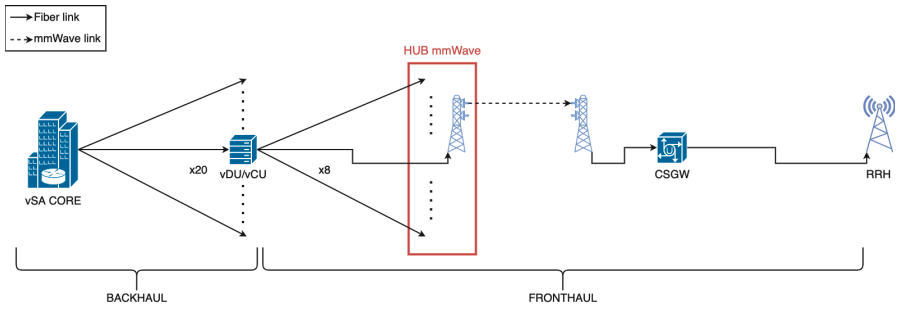

Figure 3.7: mmWave fronthauling.

we use vDU/vCU and vCORE instead of BBU, OAN and COGW. Following this approach the consumption of these apparatus is:

$$P_{\text{vDU/vCU,f}} = N_{\text{vDU/vCU,f}} P_{\text{vDU/vCU}}, \tag{3.39}$$

and

$$P_{\text{vCORE,f}} = N_{\text{vCORE,f}} P_{\text{vCORE}}, \tag{3.40}$$

respectively. The term $N_{\text{vDU/vCU,f}}$, which represent the number of vDU/vCU, is computed as:

$$N_{\text{vDU/vCU,f}} = \lceil N_{\text{m}}^{5G}/8 \rceil, \tag{3.41}$$

and the number of vCORE is:

$$N_{\text{vCORE,f}} = \lceil N_{\text{vDU/vCU,f}}/20 \rceil, \tag{3.42}$$

Optical fiber fronthauling and backhauling

In Figure 3.8 we can observe the architecture of this scenario. As we can see each building is equipped with at least one vDU/vCU that is connected via fiber links to the ONU and finally to each station. Here the power consumed by each station can be computed as:

$$P_{\text{f}}^{5G} = P_{\text{RRH,f}}^{5G} + P_{\text{ONU}} + 2P_{\text{OPT}}. \tag{3.43}$$

Thus the overall consumption becomes:

$$P_{\text{f,opt}}^{5G} = N_{\text{f}}^{5G} P_{\text{f}}^{5G} + P_{\text{vDU/vCU,f}} + P_{\text{vCORE,f}} \tag{3.44}$$

where P_{ONU} represent the power consumed by the ONU, N_{f}^{5G} is the number of femtocell calculated as in the previous cases.

Radio link backhauling and copper fronthauling

In this case, we assume that the buildings' roof are equipped with a mmWave P2P antenna, which is connected to an aggregation hub. Femtocells are connected to an Ethernet switch positioned on the roof close to the receiving antenna which is connected to the vDU/vCU, while mmWave hub are connected

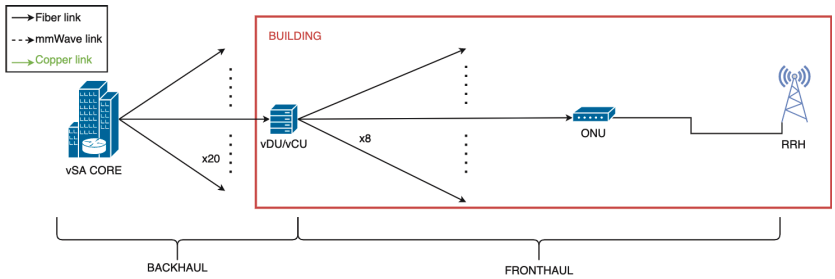

Figure 3.8: Optical fiber fronthauling and backhauling.

to the backbone via the vCORE. Assuming $N_{\mathrm{H,L,f}} = 8$, we compute the hub contribution in the same way as in the microcell:

$$P^{5G}_{\mathrm{H,f}} = N^{5G}_{\mathrm{H,L,f}} \left(P_{\mathrm{P2P}} + P_{\mathrm{OPT}}\right) \tag{3.45}$$

Moreover there are two additional terms due to mmWave P2P links which are:

$$P^{5G}_{\mathrm{ROOFS}} = N^{5G}_{\mathrm{b}} \left(P_{\mathrm{P2P}} + P_{\mathrm{OPT}}\right), \tag{3.46}$$

and

$$P^{5G}_{\mathrm{BUILDINGS}} = N^{5G}_{\mathrm{b}} \left(2P_{\mathrm{OPT}} + P_{\mathrm{GES}}\right). \tag{3.47}$$

Here N^{5G}_{b} is the number of buildings and P_{GES} in the consumption of a GES.

In this scenario the consumption of a femtocell becomes:

$$P^{5G}_{\mathrm{f}} = P^{5G}_{\mathrm{RRH,f}} + P_{\mathrm{ETH}} + 2P_{\mathrm{CU}}. \tag{3.48}$$

Hence the overall consumption is:

$$P^{5G}_{\mathrm{f,MW}} = N^{5G}_{\mathrm{f}} P^{5G}_{\mathrm{f}} + P^{5G}_{\mathrm{ROOFS}} + P^{5G}_{\mathrm{BUILDINGS}} + P^{5G}_{\mathrm{H,f}} N^{5G}_{\mathrm{H,f}} + P_{\mathrm{vDU/vCU,f}} + P_{\mathrm{vCORE,f}} \tag{3.49}$$

where the number of hub is:

$$N^{5G}_{\mathrm{H,m}} = \lceil N^{5G}_{\mathrm{f}} / N^{5G}_{\mathrm{H,L,m}} \rceil; \tag{3.50}$$

Copper fronthauling

This scenario shares the same topology as the microwave scenario, which remains exactly the same except for the P2P links that are substituted by optical fiber, as we can see in Figure 3.10. The network consumption is obtained as:

$$P^{5G}_{\mathrm{f,CU}} = N^{5G}_{\mathrm{f}} P^{5G}_{\mathrm{f}} + P^{5G}_{\mathrm{BUILDINGS}} + P_{\mathrm{vDU/vCU,f}} + P_{\mathrm{vCORE,f}} \tag{3.51}$$

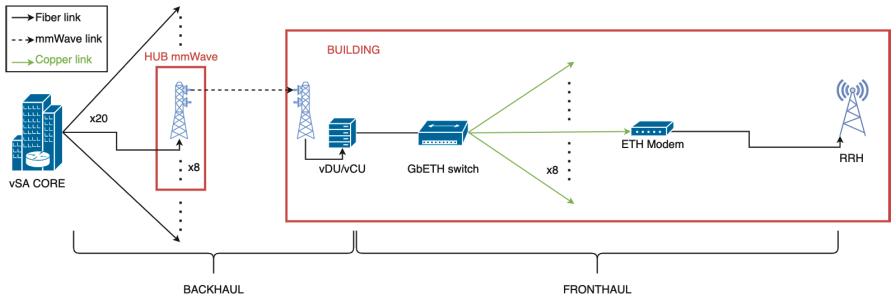

Figure 3.9: mmWave backhauling and copper fronthauling.

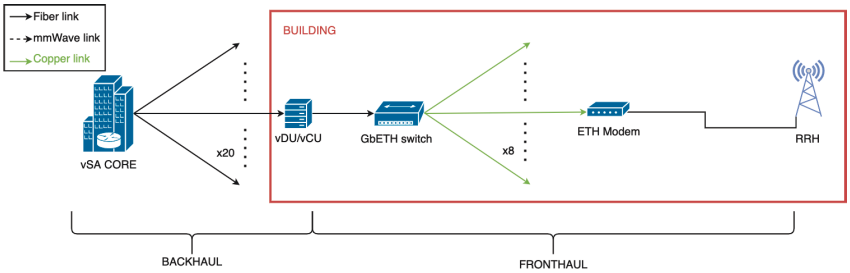

Figure 3.10: Optical fiber backhauling and copper fronthauling.

3.3.4 Fixed Architecture Modeling

As we have done for the 4G scenario we analyzed also for 5G the impact of varying the transmitted power of the stations when the network architecture is fixed. Just like before, the power needed at the transmitters to satisfy the traffic demand is modeled following the Shannon–Hartley theorem for channel capacity via this formula:

$$C = BN_{\text{sec}}N_{\text{ant}}log_2(1 + SNR). \tag{3.52}$$

where C is the channel capacity in Mbps, B is the channel bandwidth in Hertz, N_{sec} is the number of sectors in a given cell, N_{ant} is the number of antennas in a sector and SNR is the signal-to-noise ratio at the receiver.The relationship between the transmitted power and the power consumed by the cell is provided in [20], and it is:

$$P_{\text{RRH}}^{5G} = N_{\text{sec}}\left(P_{\text{TX}}/\epsilon + N_{\text{ant}}P_{\text{C}} + P_{\text{B}}\right), \tag{3.53}$$

where N_{sec} is the number of sectors, P_{TX} is the trasmitted power obtained by the previous formula, ϵ is the power amplifier efficiency, N_{ant} is the number of antennas in a sector, P_{C} is circuit power per RF branch and P_{B} is the baseline power for 5G. This formula is assumed to be valid in all scenarios except for macrocells when they are in idle where it is replaced by:

$$P_{\text{RRH}}^{5G} = N_{\text{sec}}\delta P_{\text{B}}, \tag{3.54}$$

in which δ represents the 5G sleep factor. For the macrocells the value of P_{B} is known while for microcells and femtocells is calculated by inverting 3.53 knowing the maximum consumption of a RRH.

3.3.5 Hybrid Urban scenario

As seen for 4G in real urban scenarios, hybrid solutions that mix macrocells, microcells and pico/femtocells are deployed. To account for this, we consider two urban scenarios where the macrocells and microcells are deployed beside the femtocells, respectively. The degree of femtocells versus macro- and microcells is determined, just like before, by the femtocell penetration parameter η, as in [2], ranging between 0 and 1, trivially meaning no femtocells deployed or only femtocell deployed, respectively.

The equations that rule this scenario are the same as the previous scenarios. Hence, the network power consumption in the case of macrocell hybrid scenario is computed as:

$$P^{5G}_{\mathrm{HYB,M,x}} = P^{5G}_{\mathrm{M,x}} + P^{5G}_{\mathrm{f,y}}, \tag{3.55}$$

where x and y define the possible back- and fronthauling technologies. In particular, we consider the (x, y) combinations $(\mathrm{MW}, \mathrm{MW})$, $(\mathrm{MW}, \mathrm{CU})$ and $(\mathrm{opt}, \mathrm{opt})$. The same holds for the microcell:

$$P^{5G}_{\mathrm{HYB,m,x}} = P^{5G}_{\mathrm{m,x}} + P^{5G}_{\mathrm{f,y}}. \tag{3.56}$$

3.4 5G mmWave Network Architectures

When considering the 5G technologies we took into account also for millimeter wave so for frequencies above 24 GHz. In particular we found interest in two types of cells which operate in this spectrum: street macros and femtocells. The former is a device that can be compared to the microcells seen before in term of area covered, while the latter follows the same approach as before.

3.4.1 StreetMacro cell

According to [19], we define StreetMacro cells as cellular NAP that can provide connectivity up to $C_{\mathrm{SM,max}} = 5200$ [Mbit/s], while having a coverage area up to 2.6 Km^2 as per [21] . The power consumption of a StreetMacro can be computer as:

$$P^{mmW}_{\mathrm{SM}} = P^{mmW}_{\mathrm{BBU,SM}} + P^{mmW}_{\mathrm{RRH,SM}}, \tag{3.57}$$

where $P^{5G}_{\mathrm{BBU,SM}}$ indicates the power consumed by the StreetMacro Base Band Unit (BBU) and $P^{5G}_{\mathrm{RRH,SM}}$ is the Remote Radio Head (RRH) power consumption required to guarantee the full throughput.

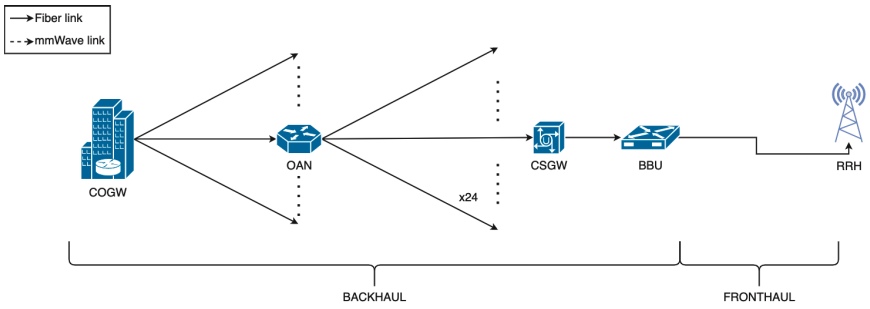

Figure 3.11: Optical fiber backhauling.

Optical fiber backhauling

From Figure 3.11 we can observe that we are facing with the same topology as the 5G macrocell scenario, with the difference that in this case each OAN can serve up to $N^{mmW}_{\text{SUB,SM}} = 24$ StreetMacro, so the overall power consumption is:

$$P^{mmW}_{\text{SM,opt}} = N^{mmW}_{\text{SM}} \left(P^{mmW}_{\text{SM}} + P_{\text{CSGW}} + P_{\text{OPT}}\right) + N^{mmW}_{\text{OAN,SM}} \left(P^{mmW}_{\text{OAN}} + P_{\text{OPT}} N^{mmW}_{\text{SUB,SM}}\right) + N^{mmW}_{\text{COGW,M}} P_{\text{COGW}}, \quad (3.58)$$

where P_{CSGW}, P^{mmW}_{OAN}, P_{COGW} represent the power consumed by the optical CSGW, the OAN and the COGW, respectively, while P_{OPT} is the power consumed by the optical link, according to the standards in 2.1. Lastly, N^{mmW}_{SM} is the total number of StreetMacro cells in the network, computed as seen before with this approach and $N^{mmW}_{\text{COGW,M}} = \lceil N^{mmW}_{\text{OAN,SM}} / N_{\text{AGG}}$ is the number of COGW;

$$N^{mmW}_{\text{SM}} = \left.\frac{(1-\eta)\,\tau}{C_{\text{SM,max}}}^{5G}\right|_{\eta=0}, \quad (3.59)$$

Lastly, observe that $N^{mmW}_{\text{OAN,SM}} = \lceil N^{mmW}_{\text{SM}} / N^{mmW}_{\text{SUB,SM}} \rceil$.

Radio link backhauling

As with the Optical Fiber backhauling this scenario follows the architecture seen in 5G macrocells with the only differences being the number of Streetmacro cells per aggregator and the number of StreetMacro served by an hub which is $N^{mmW}_{\text{H,L,SM}} = 8$ in order to have an integer number of input to for the OAN.

The hub power consumption can be computed as:

$$P^{mmW}_{\text{H,SM}} = N^{mmW}_{\text{H,L,SM}} \left(P_{\text{P2P}} + P_{\text{OPT}}\right) \quad (3.60)$$

where P_{P2P} is the power used by a single millimiter wave radio. Considering the whole network architecture, shown in Figure 3.12, we have:

$$P^{mmW}_{\mathrm{SM,MW}} = N^{mmW}_{\mathrm{SM}} \left(P^{mmW}_{\mathrm{SM}} + P_{\mathrm{CSGW}} + P_{\mathrm{P2P}} + 2P_{\mathrm{OPT}}\right) + N^{mmW}_{\mathrm{OAN,SM}} \left(P^{mmW}_{\mathrm{OAN}} + P_{\mathrm{OPT}} N^{mmW}_{\mathrm{SUB,SM}}\right) + N^{mmW}_{\mathrm{H,SM}} P^{mmW}_{\mathrm{H,SM}} + N^{mmW}_{\mathrm{COGW,M}} P_{\mathrm{COGW}}, \quad (3.61)$$

which compared to the previous case include the added contributions of the millimeter wave hubs and radios plus the additional optical ports required. In particular, $N^{mmW}_{\mathrm{H,SM}}$ is the number of millimeter wave hubs required for the network and is equal to:

$$N^{mmW}_{\mathrm{H,SM}} = \lceil N^{mmW}_{\mathrm{SM}} / N^{mmW}_{\mathrm{H,L,SM}} \rceil; \quad (3.62)$$

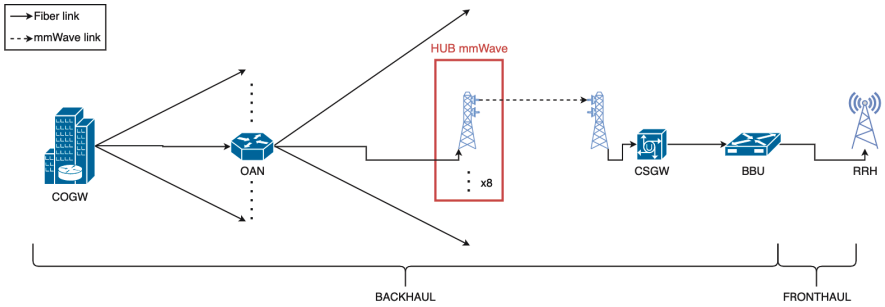

Figure 3.12: mmWave backhauling.

3.4.2 Femtocell

This scenario is very similar to the one seen in 4G case with the change in the OAN seen before. Moreover in this case the power consumption of a femtocell includes both the BBU and the RRH and is equal to P^{mmW}_{femto}.

Optical fiber fronthauling

With optical fiber fronthauling, shown in Figure 3.13, femtocells are feeded by an ONU that receives an optical fiber from the OAN which serves $N^{mmW}_{\mathrm{SUB}} = 24$ cells, and is then connected to the backbone via the COGW. As a result, the overall network consumption is:

$$P^{mmW}_{\mathrm{f,opt}} = N^{mmW}_{\mathrm{f}} \left(P^{mmW}_{\mathrm{femto}} + P_{\mathrm{ONU}} + P_{\mathrm{OPT}}\right) + N^{mmW}_{\mathrm{OAN,f}} \left(P^{mmW}_{\mathrm{OAN}} + P_{\mathrm{OPT}} N^{mmW}_{\mathrm{SUB,f}}\right) + N^{mmW}_{\mathrm{COGW,f}} P_{\mathrm{COGW}}, \quad (3.63)$$

where N^{mmW}_{f} is the number of femtocells calculated as seen for the other scenarios, $N_{\mathrm{SUB,f}}$ is the same as in StreetMacro and finally we can see that $N^{mmW}_{\mathrm{OAN,f}} = \lceil N^{mmW}_{\mathrm{f}} / N^{mmW}_{\mathrm{SUB,f}} \rceil$ and $N^{5G}_{\mathrm{COGW,f}} = \lceil N^{mmW}_{\mathrm{OAN,f}} / N_{\mathrm{AGG}}$.

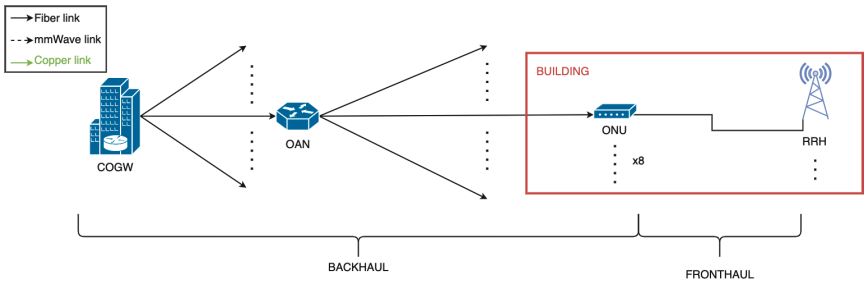

Figure 3.13: Optical fiber fronthauling.

Radio link backhauling

In the case of radio backhaul, as we can see from Figure 3.14 each cell is connected to a Ethernet modem and via copper cables to a gigabit Ethernet switch that is positioned on the roof of the building where there is a mmWave P2P antenna that communicates with a mmWave hub that is directly linked to the OAN via various optical fiber links and finally to the COGW. In order to compute the overall consumption we need to introduce three components:

$$P_{\text{ROOFS}}^{mmW} = N_{\text{b}}^{mmW} \left(P_{\text{P2P}} + P_{\text{OPT}}\right), \tag{3.64}$$

$$P_{\text{BUILDINGS}}^{mmW} = N_{\text{b}}^{mmW} \left(P_{\text{OPT}} + P_{\text{GES}}\right). \tag{3.65}$$

and

$$P_{\text{H,f}}^{mmW} = N_{\text{H,L,f}}^{mmW} \left(P_{\text{P2P}} + P_{\text{OPT}}\right) \tag{3.66}$$

Here N_{b}^{mmW} is the number of buildings which is the same as before and $N_{\text{H,L,f}}^{mmW}$ is equal to 3. Hence, the overall consumption can be computed as:

$$\begin{aligned} P_{\text{f,MW}}^{mmW} &= N_{\text{f}}^{mmW} \left(P_{\text{f}}^{mmW} + P_{\text{ETH}} + 2P_{\text{CU}}\right) \\ &\quad + P_{\text{ROOFS}}^{mmW} + P_{\text{BUILDINGS}}^{mmW} + N_{\text{OAN,f}}^{mmW} \left(P_{\text{OAN}}^{mmW} + P_{\text{OPT}} N_{\text{SUB,f}}^{mmW}\right) \\ &\quad + N_{\text{H,f}}^{mmW} P_{\text{H,f}}^{mmW} + N_{\text{COGW,f}}^{mmW} P_{\text{COGW}}, \end{aligned} \tag{3.67}$$

where $N_{\text{SUB,f}}^{mmW} = 3$ is the number of links per OAN and $N_{\text{H,f}}^{mmW} = \lceil N_{\text{f}}^{mmW} / N_{\text{H,L,f}}^{mmW} \rceil$.

Copper backhauling

This scenario shares the same architecture with the radio link one with the exception of the mmWave P2P links which are removed, as can be seen in Figure 3.15. In this case the total power consumption becomes:

$$\begin{aligned} P_{\text{f,CU}}^{mmW} &= N_{\text{f}}^{mmW} \left(P_{\text{f}}^{mmW} + P_{\text{ETH}} + 2P_{\text{CU}}\right) \\ &+ P_{\text{BUILDINGS}}^{mmW} + N_{\text{OAN,f}}^{mmW} \left(P_{\text{OAN}}^{mmW} + P_{\text{OPT}} N_{\text{SUB,f}}^{mmW}\right) + N_{\text{COGW,f}}^{mmW} P_{\text{COGW}}. \end{aligned} \tag{3.68}$$

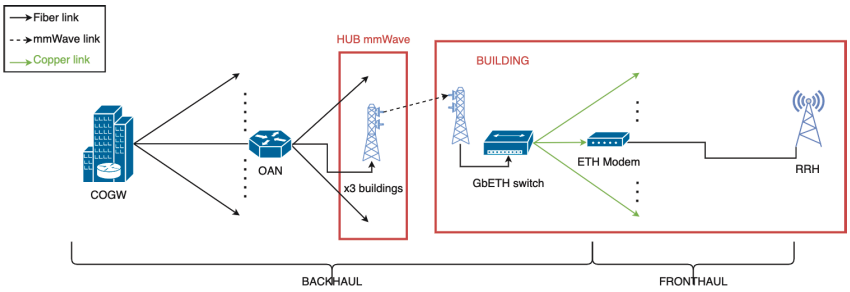

Figure 3.14: mmWave backhauling.

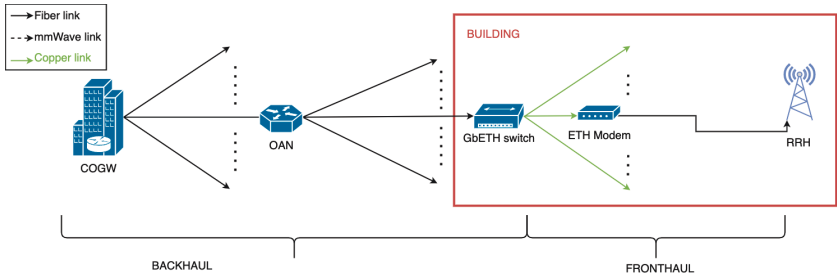

Figure 3.15: Copper backhauling.

3.4.3 Fixed Architecture Modeling

For the simulation of the variations of overall power when the network dimensions are fixed and the traffic demand changes we used the same relations shown in 3.3.4 for the case of microcells and femtocells.

3.4.4 Hybrid Urban scenario

The same said in the previous section applies also here, in fact we used the approach from 5G scenarios in the case of microcells and femtocells. Hence the corresponding total power consumption becomes:

$$P^{5G}_{\mathrm{HYB,m,x}} = P^{mmW}_{\mathrm{SM,x}} + P^{mmW}_{\mathrm{f,y}}. \tag{3.69}$$

where x and y define the possible back- and fronthauling technologies. In particular, we consider the (x, y) combinations $(\mathrm{MW}, \mathrm{MW})$, $(\mathrm{MW}, \mathrm{CU})$ and $(\mathrm{opt}, \mathrm{opt})$.

Chapter 4

Model database

The model database collects the data obtained from the literature, commercial device data sheets and telco data that were collected in the phase 3 of the study. Every number is reported with its primary source.

4.1 Network data

Network data for the 4G scenarios were obtained from [15], gathered from actual architectures over a portion of the aggregation infrastructure owned by the operator Orange. Specifically, the authors consider a 15 Km^2 coverage area, centered in one of the top-ten French cities, as representative of a typical urban area, and comprising 86 macrocells, 13 aggregation nodes and one COGW. Numbers are provided for several architectural solutions, including those considered in the study. In particular, we refer to the d-BS/PtP solution as it provides the average performance in terms of fiber length and power consumption. To validate the model, we check that our results match the numbers in [15]. On the other hand, for the 5G scenarios there isn't enough data available at the moment, particularly for mmWave wave networks. For this reason in our simulations we used the data obtained from the data sheets of the devices and from the assumptions that we have made.

4.2 Cell data

Cell data were gathered from independent sources cited in Table 4.1. To validate the numbers provided in literature, which are mostly nominal working values, we referred to [18]. The paper provides power consumption measurements of macrocells and microcells retrieved by in-site measurements, which align to the values that were used for the simulation.

ID	Parameter	Value	Reference
1	$P^{4G}_{\mathrm{RRH,M}}$	350	[15–17]
2	$P^{4G}_{\mathrm{BBU,M}}$	250	[15]
3	$P^{4G}_{\mathrm{max,M}}$	40	[16, 17]
4	$P^{4G}_{\mathrm{RRH,m}}$	86	[16, 17]
5	$P^{4G}_{\mathrm{BBU,m}}$	68.8	[16, 17]
6	$P^{4G}_{\mathrm{RRH,p}}$	8.7	[16, 17]
7	$P^{4G}_{\mathrm{BBU,p}}$	6	[16, 17]
8	$P^{4G}_{\mathrm{RRH,f}}$	1	[22]
9	$P^{4G}_{\mathrm{BBU,f}}$	5	[16, 17]
10	P^{4G}_{link}	22	[16]
11	$N_{\mathrm{sec,M}}$	3	[15, 16]
12	$N^{4G}_{\mathrm{ant,M}}$	2	[15, 16]
13	$N^{4G}_{\mathrm{ant,m}}$	2	[15, 16]
14	$\Delta^{4G}_{\mathrm{loss,M}}$	1.24	[16]
15	$\Delta^{4G}_{\mathrm{loss,m}}$	1.15	[16]
16	$\Delta^{4G}_{\mathrm{loss,f}}$	1.10	[16]

Table 4.1: 4G Aggregated cell data.

ID	Parameter	Value	Reference
1	$P^{5g}_{\mathrm{RRH,M}}$	4200	[1]
2	$P^{5G}_{\mathrm{BBU,M}}$	500	[1]
3	$P^{5G}_{\mathrm{max,M}}$	50	[23]
4	$N^{5G}_{\mathrm{ant,M}}$	64	[1]
5	$P^{5G}_{\mathrm{RRH,m}}$	450	[24]
6	$P^{5G}_{\mathrm{max,m}}$	20	[25]
7	$N^{5G}_{\mathrm{ant,m}}$	4	[26]
8	$P^{5G}_{\mathrm{RRH,f}}$	60	[27]
9	$P^{5G}_{\mathrm{max,f}}$	0.1	[25]
10	$N^{5G}_{\mathrm{ant,f}}$	4	[27]

Table 4.2: 5G Aggregated cell data.

ID	Parameter	Value	Reference
1	$P^{mmW}_{\mathrm{RRH,SM}}$	300	[28]
2	$P^{mmW}_{\mathrm{BBU,SM}}$	310	[29]
3	$P^{mmW}_{\mathrm{max,SM}}$	20	[25]
4	$N^{mmW}_{\mathrm{ant,SM}}$	4	[28]
5	P^{mmW}_{femto}	50	[30]
7	$P^{mmW}_{\mathrm{max,f}}$	0.1	[25]
8	$N^{mmW}_{\mathrm{ant,f}}$	4	[30]

Table 4.3: 5G mmWave Aggregated cell data.

ID	Parameter	Value [W]	Reference
1	$P_{\text{COGW,1}}$ (48 port)	170	[15]
2	$P_{\text{COGW,2}}$ (96 port)	223	[15]
3	P_{COGW}	196.5	Average of 1-2
4	$P_{\text{CSGW,1}}$	20	[15]
5	$P_{\text{CSGW,2}}$	300	[2]
6	P_{CSGW}	160	Average of 4-5
7	P_{DSL}	85	[2]
8	P_{GES}	50	[2]
9	P_{ETH}	5	[2]
10	P_{CU}	3.5	[2]
11	P_{ONU}	4	[2]
12	P_{SFP}	1	[2]
13	$P_{\text{SFP+}}$	1.5	[2]
14	P_{XFP}	0.7	[15]
15	P_{QSFP}	4	[15]
16	P_{OPT}	1.8	Average of 12-15
17	PL-1000TE	120	[4]
18	PL-2000	68	[4]
19	PL-2000AD	350	[4]
20	PL-2000ADS	170	[4]
21	PL-2000T	250	[4]
22	P_{OAN}	191.6	Average of 17-21
23	P_{OAN}^{mmW}	517	[31]
24	P_{P2P}	58	[6]
25	$P_{\text{vDU/vCU}}$	280	[32, 33]
26	P_{vCORE}	280	[34, 35]

Table 4.4: Device data.

4.3 Device data

As for the cell data, device data were collected from independent sources. We report the values with sources in Table 4.4.

4.4 Environment data

Environment data were collected from [36], (4) and (5). They are reported in Table 4.5. Finally, in order to estimate the network bandwidth demand we assume that the population is divided into 2 types of users, namely heavy and normal users. The difference between the two types is that normal users consume 8 times less data as the heavy users [2]. Moreover, users are assumed to be using 3 types of devices: smartphones, tablets and laptops. Each of these devices is assumed to consume 0.185, 1.55 and 9 Mbps, respectively, when used

by heavy users. The devices are assumed to be used by 85%, 50% and 25% of the population, respectively, so that scenarios with users equipped with multiple active devices are considered.

Scenario	Population density [people/Km^2]	Building density [buildings/Km^2]	Area size [Km^2]	N° apartments per building
Urban	3000	250	181	10
Sub-urban	600	178	1500	2
Rural	93	25	1000	2

Table 4.5: Environment data.

4.5 Radio access network data

In our model, Sub-6GHz are considered not only for backhauling but also for the radio access network (hence macrocells, microcells and femtocells) in every 4G and 5G scenario, while 5G mmWave uses frequencies above 6 Ghz. For our simulation we used the following specifications for the actual devices, obtained by their respective datasheets:

- for the 4G scenario, we assume that the spectrum bandwidth occupied by a given cell is 20 MHz in the range 700-2600 MHz, according to [37]. In particular, for macrocell and microcells we considered band 3, at 1800 MHz, with 2x2 MIMO and 1x1 SISO antennas, respectively. Instead, for femtocells we opted for band 7, at 2600 MHz, with 1x1 SISO antennas. In all the architectures the modulation used for the down-link is 256 QAM, which guarantees, in conjunction with the antennas used, speeds of 200 Mbps in case of macrocells and 100 Mbps in the other architectures.

- for the 5G case, we assume that the spectrum bandwidth occupied by a given cell is 100 MHz in the range 700-4900 MHz according to [38], [26], [27]. In particular, for macrocell we considered band 79, at 4500 MHz, with 64x64 massive MiMo while for microcells and femtocells we opted for band 78, at 3500 MHz, with 4x4 antennas, respectively. In all the architectures the modulation used for the down-link is 256 QAM, which guarantees, in conjunction with the antennas used, speeds of 1800 Mbps in case of macrocells [19] and 1250 Mbps in the other architectures.

- for the 5G mmWave simulation, we assume that StreetMacros and femtocells operate in frequencies in the order of 26.5–29.5 GHz (e.g., band 258) with a bandwidth of 400 MHz and 4x4 MiMo antennas which in conjunction to a 256 QAM modulation guarantee 5200 Mbps of throughput, according to [19], in both StreetMacros and femtocells.

Chapter 5

Numerical Results

The equations provided in Chapter 3 are fed with the number of Chapter 4. For each scenario, we evaluate the power consumption as a function of the network traffic load by increasing the bandwidth demand by shifting the ratio between normal user and heavy user h_p between the two extremes. We also analyzed the impact of different network dimensions, i.e. varying the number of cells, with different level of traffic, on the overall consumption, though limitations on the number of cells per km^2 are not considered, since the focus is on the energy consumption. Nonetheless, realistic distributions of cells per km^2 are still considered. Finally, In the hybrid scenarios, power consumption is evaluated against h_p and femtocell penetration rate η, in order to account for the degree of femtocell use (i.e., from none to exclusive use). Results are gathered by scenario to evaluate the impact of both the architectural and technological choice.

5.1 4G/LTE Networks

5.1.1 Urban Scenario

Figure 5.1 shows the network requirements for all the architectures (a combination of fronthaul/backhaul and cell type), in terms of cells that need to be deployed per square kilometer, for different levels of traffic demands and the corresponding power consumption. In Figure 5.2 we evaluated the impact of different network architectures when imposing a specific level of peak traffic in the network, thus fixing the number of cells deployed. For our analysis we assumed a network build based on a peak demand of 11 Gbps/km^2, obtained by fixing the number of heavy users to the maximum, and we evaluated the power consumption when varying the actual traffic. By comparing the right side of Figure 5.1 and Figure 5.2 we can see that, except for femtocells where the coverage requirement is always more stringent than the traffic one, it is always preferable to not over-provision the network capacity, because both in the case of macrocell and microcell the high number of cell deployed is the dominant component of the overall consumption, particularly when the load is low. In

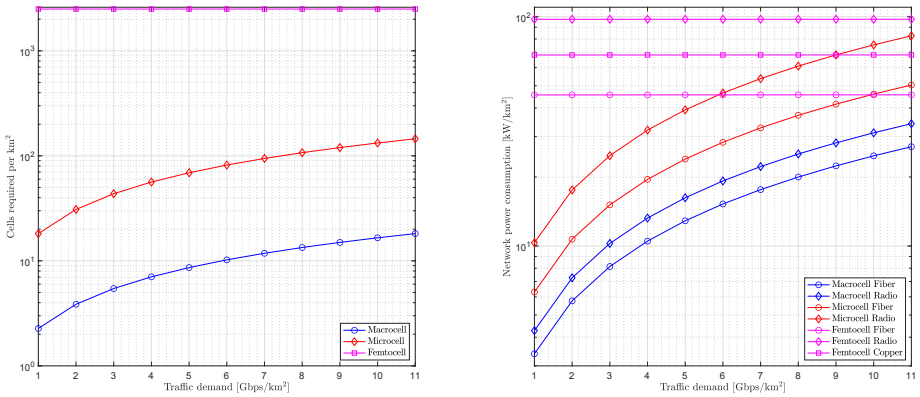

Figure 5.1: Architectures' network dimensioning and consumption, 4G/LTE Urban Scenario.

any case macrocell results to be the most convenient scenario in terms of energy consumption, as it wins the trade-off between number of deployed cells and area coverage. Microcells happen to be less energy efficient than macrocells [18], while femtocells require many deployments to provide coverage, which results in higher energy consumption. Despite the cell dimension, optical fiber results to be the winning technology in every scenario, consuming approximately 21% less power than microwave radio in macrocell scenario, while peaking at 39% and 36% in microcell and femtocell scenarios, respectively.

The breakdown of power consumption is provided in Figure 5.3, which illustrates the values corresponding to a traffic of 11 Gbps/km^2 in Figure 5.2. The following code is applied to simplify the graph notation:

- Macrocell Fiber (MF), Macrocell Radio (MR);
- Microcell Fiber (mF), Microcell Radio (MR);
- Femtocell Fiber (fF), Femtocell Radio (fR) Femtocell Copper(fC).

Figure 5.3 shows that, in the case of macrocell and microcell architecture, the highest contribution to the energy consumption is given by the backhaul network, while the fronthaul impact is almost negligible compared to the whole architecture. As long as the cell decreases in its dimension, and particularly in the femtocell case, the number of cells requested to provide coverage balances the reduced energy consumption, with negative impact on the overall network consumption. This occurs only in a small fraction due to smaller cells inefficiency (i.e., the cell itself): the main reason is the densification of the fronthaul and backhaul networks to provide connectivity to that high number of cells. Figure 5.4 provides the percentage of each contribution to the overall network consumption. Independently on the cell size, the backhaul contribution grows in all the scenarios where optical fiber is replaced with microwave and copper. This increase can be as high as 67% and 54% when switching from optical fiber

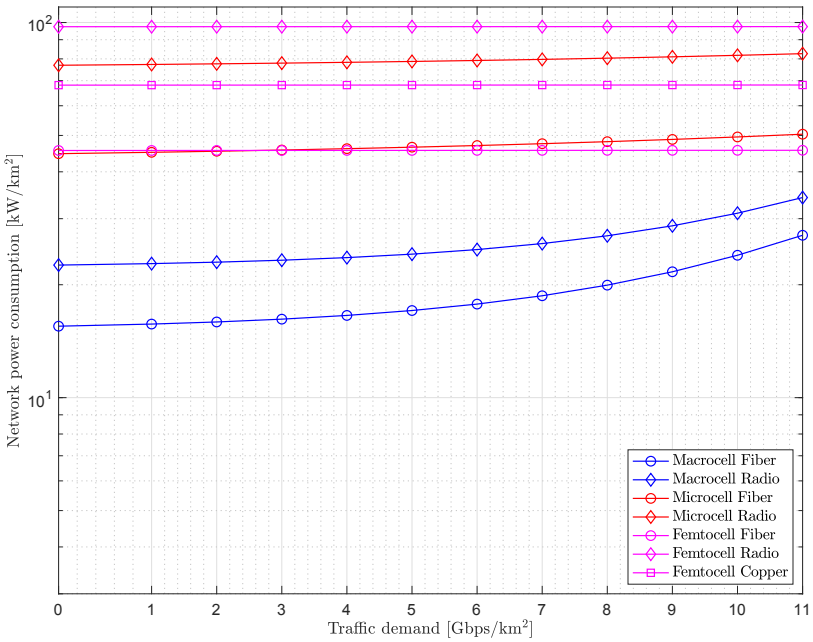

Figure 5.2: Fixed network dimensions architectures' power consumption, 4G/LTE Urban Scenario.

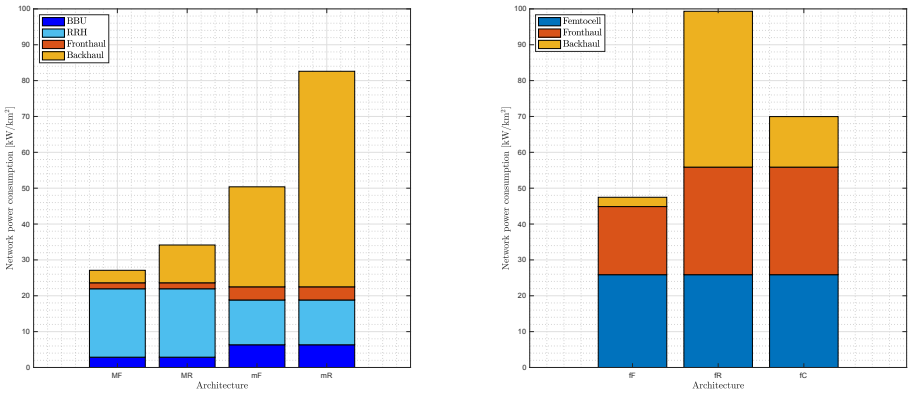

Figure 5.3: Power consumption breakdown, 4G/LTE Urban Scenario.

to microwave in macrocell and from microcell architectures, respectively, while it peaks at 94% in the case of femtocell with microwave backhaul.

5.1.2 Sub-urban Scenario

Figure 5.5 reports the results for this scenario in terms of network dimensioning and consumption. On the left there is the number of cell required for each

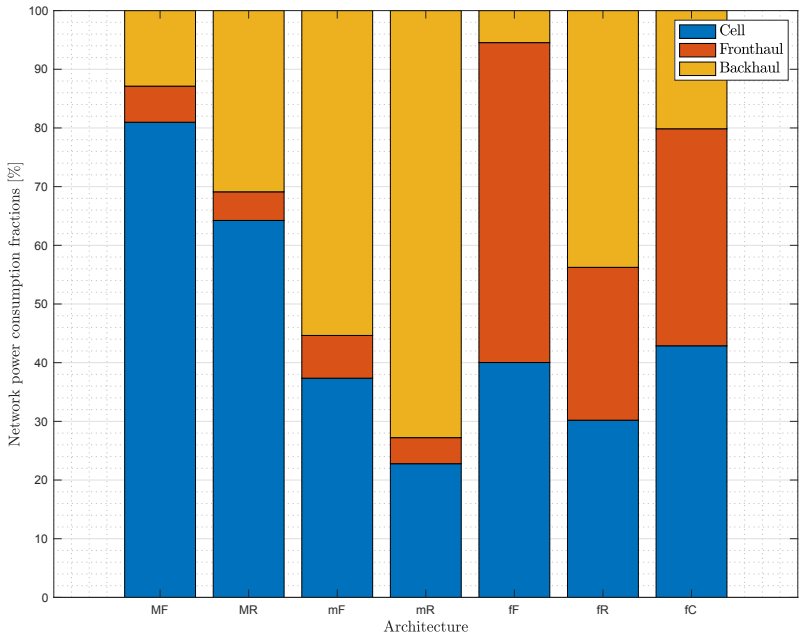

Figure 5.4: Power consumption percentages, 4G/LTE Urban Scenario.

architecture based on the traffic, while on the right we have represented the corresponding power consumption. We can see that in macrocell and microcell architectures, the comparison between optical fiber and radio provides the same results as the Urban Scenario, while in femtocells copper and radio consumes 54% and 79% more energy than fiber. Figure 5.6 shows the power consumption when we we fix the network dimension, i.e. the number of cells, to satisfy a

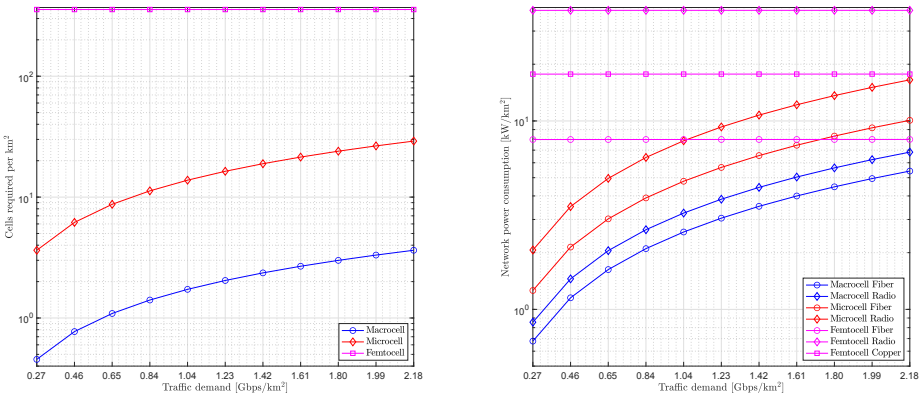

Figure 5.5: Architectures' network dimensioning and consumption, 4G/LTE Sub-urban Scenario.

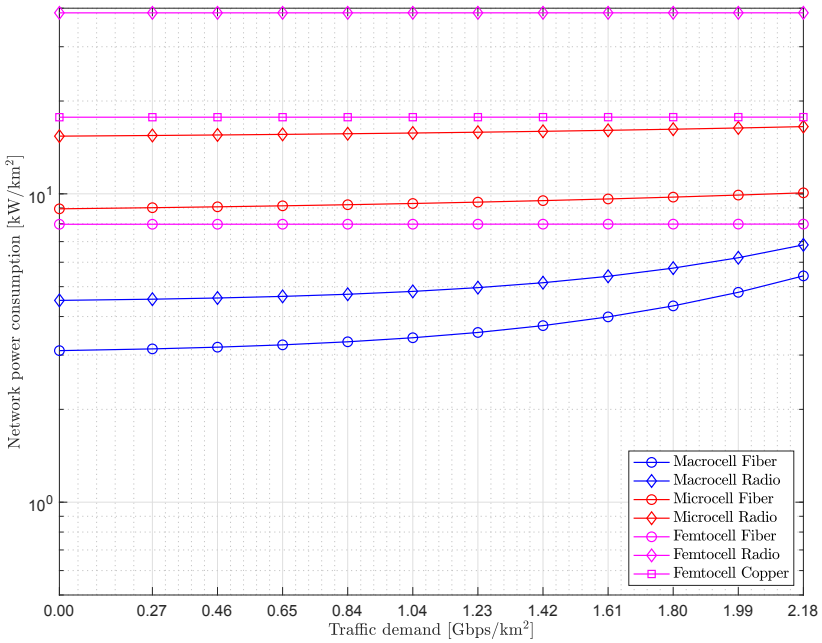

Figure 5.6: Fixed network dimensions architectures' power consumption, 4G/LTE Sub-urban Scenario.

peak traffic of 2.18 Gbps/km^2, and we vary the actual traffic. We can see that over-provisioning has the same impact as in the Urban Scenario. The power consumption breakdown with the maximum peak traffic demand is provided in Figure 5.7 and Figure 5.8 and once again, cell inefficiency plays a little role in the overall energy consumption, while the highest contribution in non-macrocell architectures is due to the backhaul. It increases, when switching from optical fiber to a non-fiber one, with percentages comparable to the previous case.

5.1.3 Rural Scenario

The results for this scenario are shown in Figure 5.9 and in Figure 5.10 and follow the same patterns as in previous cases. We observe that macrocells result to be the best options among architectures, while microwave, copper and optical fiber perform increasingly better, with optical fiber gaining up to 63% and 54% compared to microwave and copper. As seen before over-dimensioning the network leads to higher power consumption. The consumption breakdown in Figure 5.11 and Figure 5.12 shows that also for this scenario, most of the energy in micro and femtocell architectures is dedicated to backhauling. This energy consumption becomes 54% and 94% higher in microcell and femtocell architectures when switching from optical fiber to microwave, respectively, while it reaches an increase of 82% when adopting copper in the femtocell architecture.

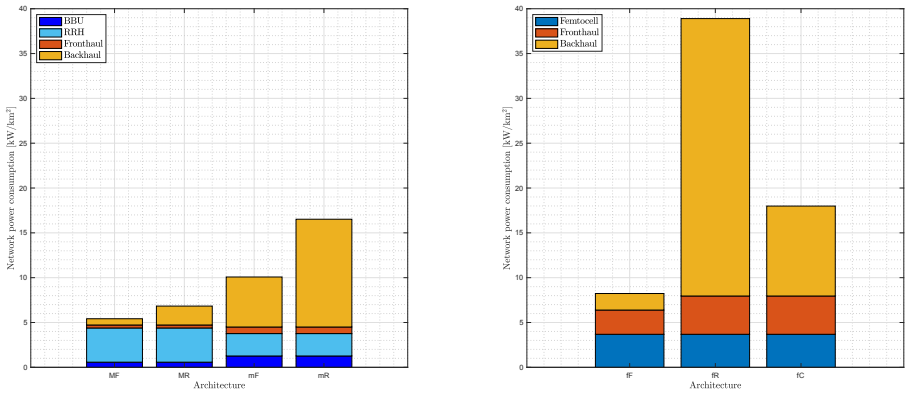

Figure 5.7: Power consumption breakdown, 4G/LTE Sub-urban Scenario.

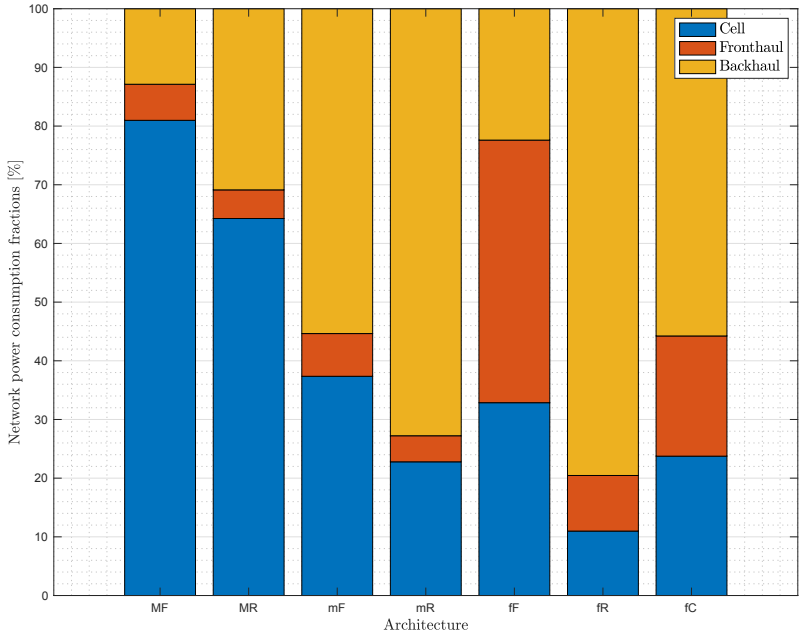

Figure 5.8: Power consumption percentages, 4G/LTE Sub-urban Scenario.

5.1.4 Hybrid Scenario

Actual architecture implementations combine the use of macrocell, microcell and femtocell to provide optimal coverage, especially in urban scenarios [18]. To address this use case, we consider a scenario where femtocell deployments are jointly set up with macrocells and microcells, while regulating the femtocell penetration by means of the parameter η.

Figure 5.13 shows the results both in the case of a fixed η, here equal to 0.5,

on the left side, and a varying one, on the right side. It can be observed that energy performance of the technologies remains the same in all the considered scenarios, not surprisingly, as the hybrid scenarios can be seen as an interpolation of the 3 scenarios explored above. This can be verified by checking the values at the extremes of Figure 5.13 (right): where $\eta = 0\%$ and $\eta = 100\%$ we have the same values of Figure 5.1 where the traffic demand is equal to 4 Gbps/km^2, while left and right sides of Figure 5.13 match at traffic demand equal to 4 Gbps/km^2 and $\eta = 50\%$ by design. We can also see that in hybrid scenarios, the differences between macrocell and microcell tend to reduce, while collapsing into the femtocell scenario. From the front- and backhauling perspective, the same conclusions derived before are still valid: microwave, copper and optical fiber perform increasingly better.

5.1.5 Real-world simulation: macrocells in Milan

In order to provide more meaningful results on the impact of different architectures, we conducted a simulation on a real world scenario, considering as an example the macrocells deployed in Milan. In particular, since detailed data on the number of cells was not available, we modeled it in the following way: we sampled three areas of the city in terms of number of macrocells for a generic operator and then we calculated the cell density in those areas, as can be seen in Table 5.1. Then we propagated the results to the whole city which we divided in three sectors, shown in Figure 5.14, that have similar characteristics to the samples, and finally, by summing up the results presented in Table 5.2 we obtained a total number of macrocell equal to 290.

Figure 5.15 shows the results in terms of power consumption variations for the considered scenario, imposing as peak traffic in the network the maximum one compatible with the number of cells, which is also used in Figure 5.16 for the power consumption breakdown. From these results we can observe that all

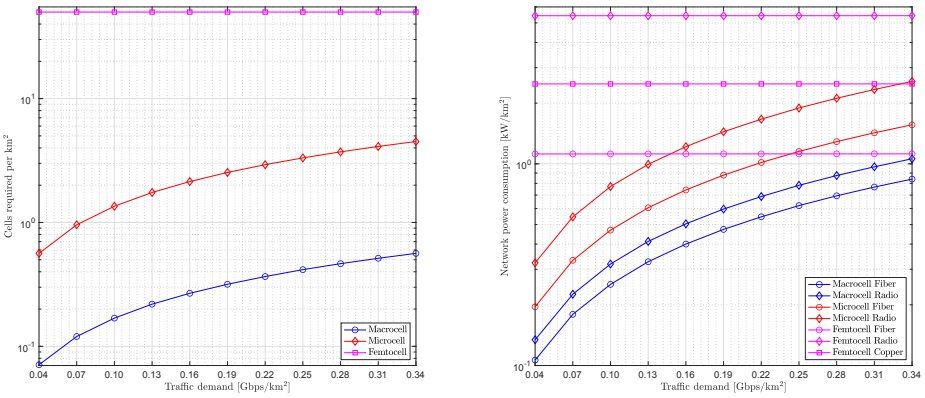

Figure 5.9: Architectures' network dimensioning and consumption, 4G/LTE Rural Scenario.

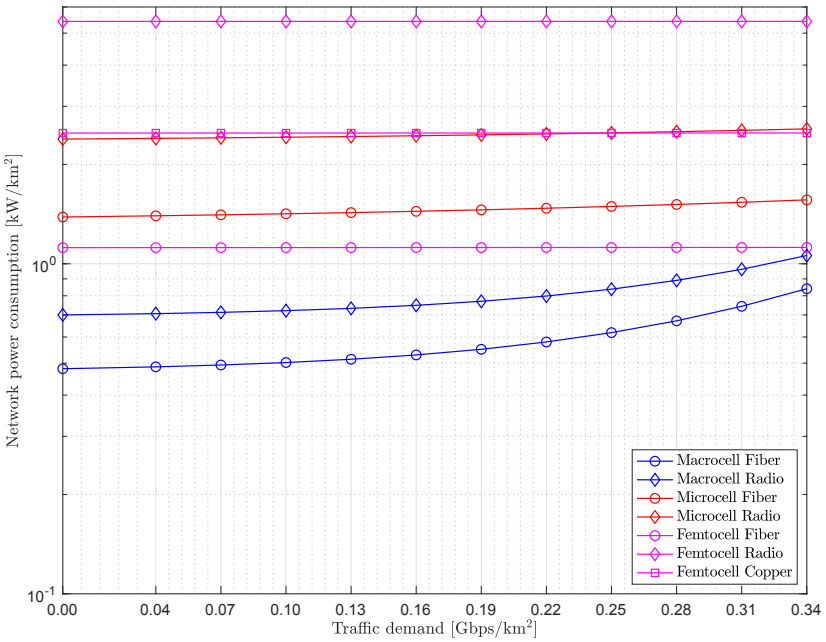

Figure 5.10: Fixed network dimensions architectures' power consumption, 4G/LTE Rural Scenario.

the previous considerations on the architectures are still valid.

In Figure 5.17 we reported the equivalent CO_2 emissions per year calculated from the consumption shown in Figure 5.16. According to [39] each kilowatt-hour in Italy creates 352 grams of CO_2, so in the case in exam switching to a fiber backhaul can reduce emissions of up to 350 tonnes per year.

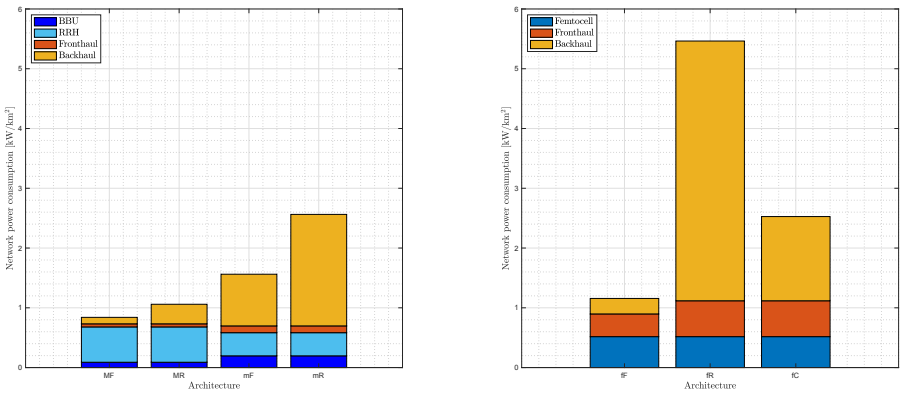

Figure 5.11: Power consumption breakdown, 4G/LTE Rural Scenario.

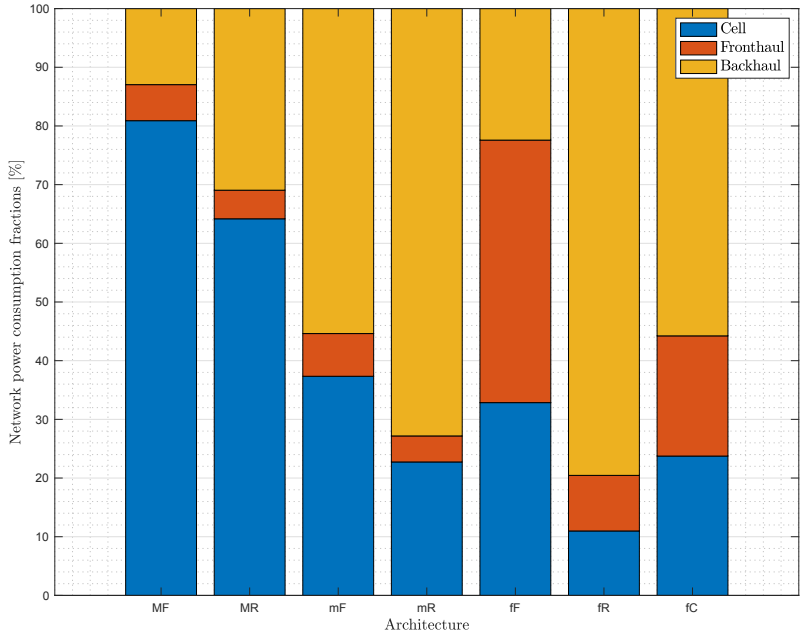

Figure 5.12: Power consumption percentages, 4G/LTE Rural Scenario.

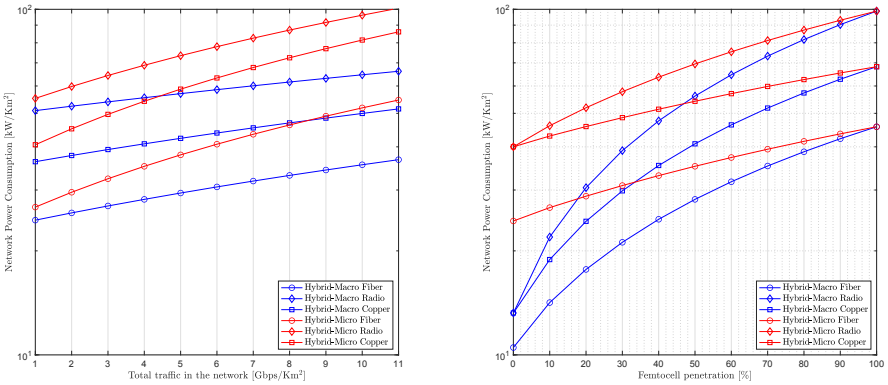

Figure 5.13: Architectures' power consumption in 4G/LTE Hybrid Scenario.

5.2 5G Sub-6GHz Networks

We now analyze the numerical results obtained for the 5G technology, considering the same scenarios and network demand as the 4G case, while integrating the architecture presented in 3.3. First, we consider sub-6 GHz technologies, including massive MIMO macrocells, 5G micro- and femtocells.

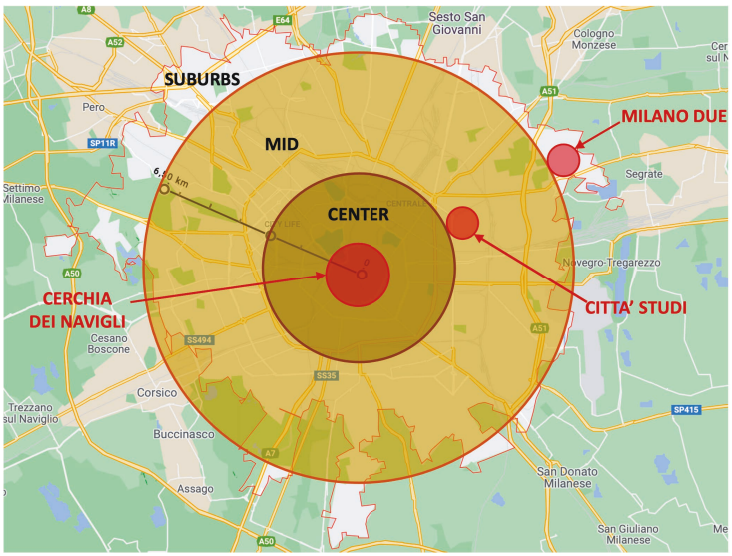

Figure 5.14: Density sectors model of Milan.

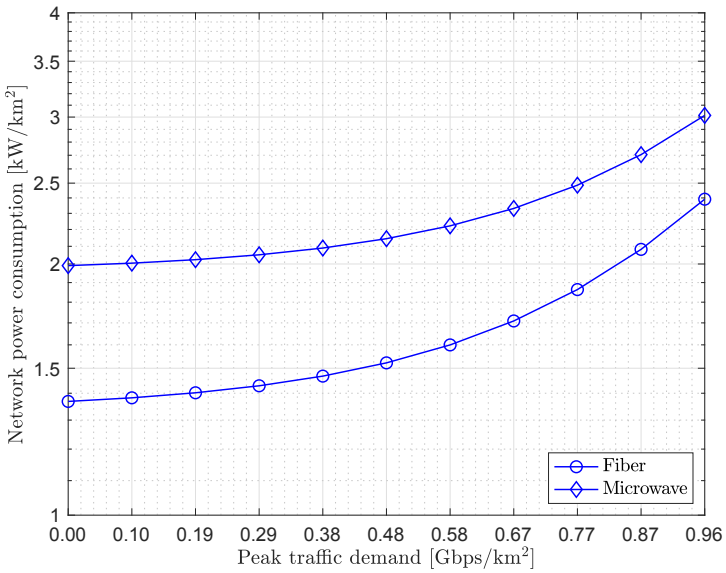

Figure 5.15: Fixed network dimensions architectures' power consumption, 4G/LTE Milan.

	Center	Mid	Suburbs
Site	Cerchia dei Navigli	Città studi	Milano Due
Area [km2]	8,2	5,87	4,42
Macrocells	26	10	2
Density [cells/km2]	3,17	1,70	0,45

Table 5.1: Sampled data

	Center	Mid	Suburbs
Ray [km]	3	6,5	-
Area [km2]	28,27	104,46	48,27
Macrocells	90	178	22

Table 5.2: Macrocell distribution results

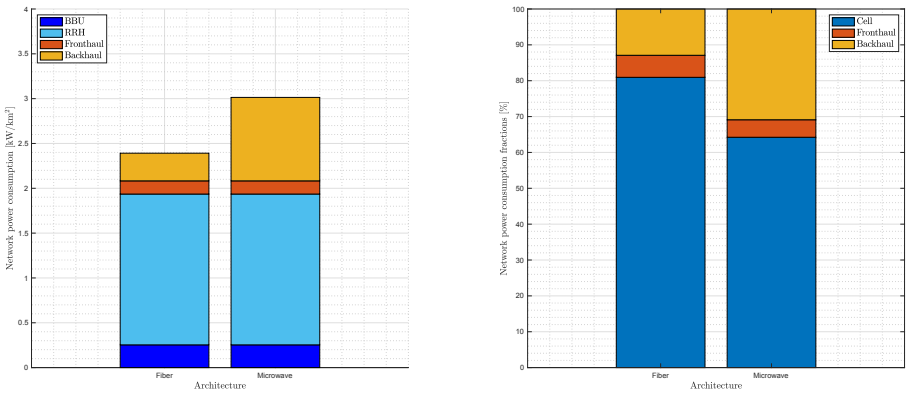

Figure 5.16: Power consumption breakdown, 4G/LTE Milan.

5.2.1 Urban Scenario

With the same driving parameters as the 4G scenario, we obtain the results of figure 5.18. We observe that femtocells, massive MIMO macrocells and microcells perform increasingly better, which results to be a major difference compared to 4G, where macrocells provided the best performance in terms of network energy consumption. Indeed, despite the smaller amount of cells per km^2 deployed, massive MIMO macrocells introduce higher energy consumption into the network compared to microcell. This is due to the combination of a higher amount of energy required to run the macrocell and a relative small gain in terms of throughput compared to the microcell, as reported in table 4.2. As expected, 5G macrocells and femocells consume more power than 4G ones, while microcells provide better performances due to a more advantageous bandwidth-energy trade off, which is remarkable. From the technology perspective, optical fiber provides better performances in all the considered scenarios, with gains up

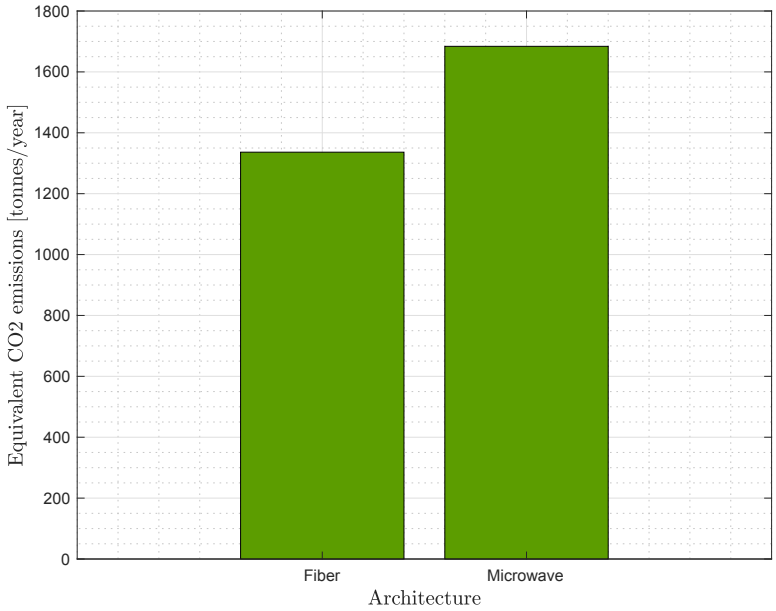

Figure 5.17: Equivalent CO_2 emissions , 4G/LTE Milan.

to 15% compared to microwave and copper, confirming the benefit found for 4G networks.

Figure 5.19 illustrates the result for a fixed network at maximum bandwidth demand, varying the required cell power according to Shannon theorem. As for 4G variation are very little when going to low power, except for the macrocell case, where we observe a small power consumption in idle state. This is expected

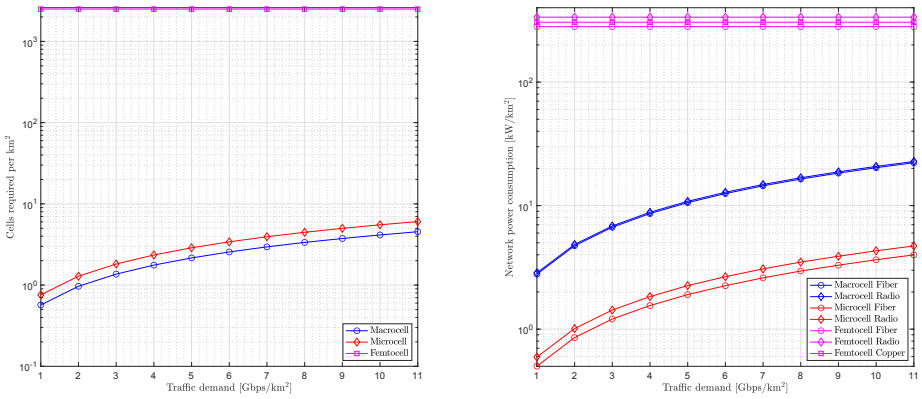

Figure 5.18: Architectures' network dimensioning and consumption, 5G Urban Scenario.

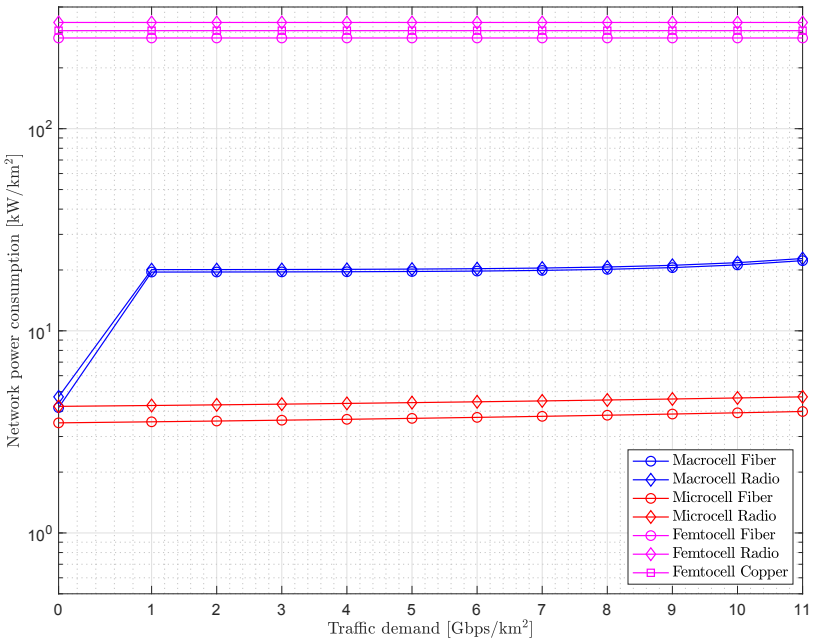

Figure 5.19: Fixed network dimensions architectures' power consumption, 5G Urban Scenario.

as the power model for the macrocell provides a discontinuity in the power profile when the macrocells enters the idle state. However, the condition to reach that state is to have no transmitted power at the antenna, which can be obtained only if no users are attached to the cell at a given instant.

Figures 5.20 and 5.21 provide the energy consumption breakdown for the scenario. We clearly see that the power consumption is dominated by the cell power consumption, which has increased by at least a factor 3 for each of the cell dimensions. However, the highest throughput allows for a reduction in the number of deployed cells, enabling a reduction in power consumption. Figure 5.20 allows to see the power distribution among the components, enhancing the fact that for increasing the cell dimensions, the cell contribution to the total network consumption grows from 10% to 90% as moving from femtocells to macrocells, compressing the back- and fronthaul contributions to a tiny amount.

5.2.2 Sub-urban Scenario

The network performance for the scenario is provided in Figure 5.22. While the overall performance is similar to the Urban scenario, we observe that for low-bandwidth requirements the number of microcell saturates to the minimum necessary to provide coverage over the interested area. This introduces a floor in the power consumption which reduces the advantage of adopting microcells

vs macrocells. However, in none of the considered points macrocells result to be more efficient than microcells. The gain provided by switching the technology from radio/copper to fiber can reach 16% and 45% in microcell and femtocell scenarios, respectively, while staying around 2% in macrocell scenarios.

Figure 5.23 implements the same equations given for 5.19, hence allows the reconstruction of the curve behind the power consumption with the growth of bandwidth demand. The same conclusions as the urban scenario hold: little to no power difference can be observed, with the exception of the notch in the macrocell scenario introduced by the equations provided in literature. Figure 5.20 and Figure 5.21 report the power consumption breakdown, reflecting the same outcome as seen in the Urban scenario as well: the highest contribution to the power consumption is represented by the cell itself for macrocell, while reduces to the front- and backhaul for the femtocell scenario. Microcells have the best trade of between the number of deployment, coverage and cell power consumption among the three options. Technology options, i.e., fiber, copper and microwave, perform increasingly better.

5.2.3 Rural Scenario

On the contrary to the previous scenarios, Figure 5.26 shows that macrocells can be convenient when the network demand decreases significantly and the area to be covered grows to several km^2. We observe a better performance in low bandwidth regime due to a smaller deployment of cells in the area, while the number of microcells to be deployed is dominated by dimensions of the area to be covered.

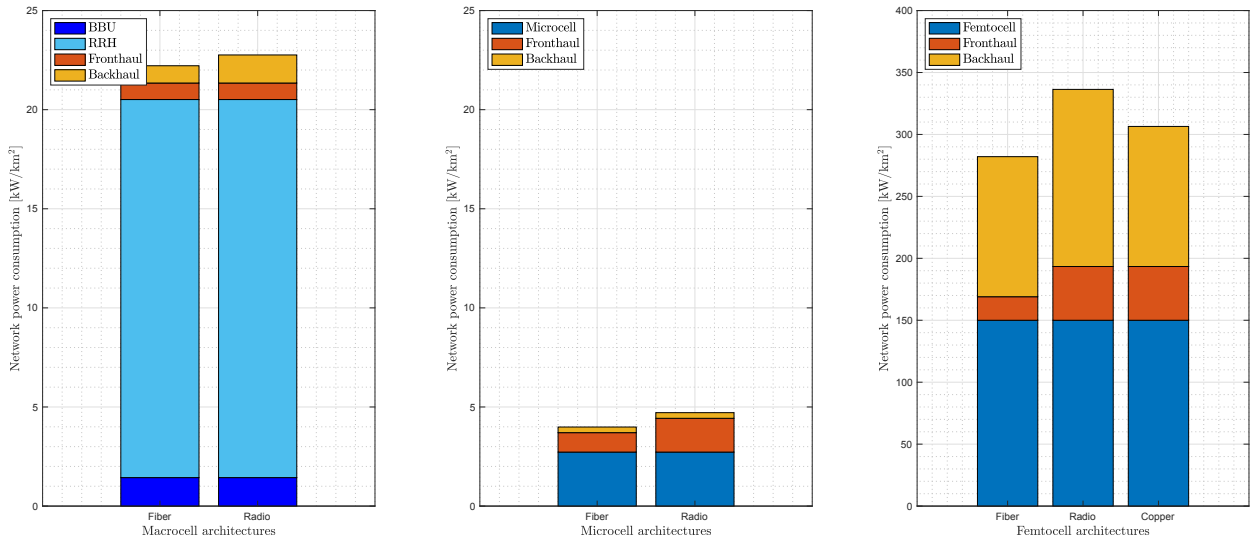

Figure 5.20: Power consumption breakdown, 5G Urban Scenario.

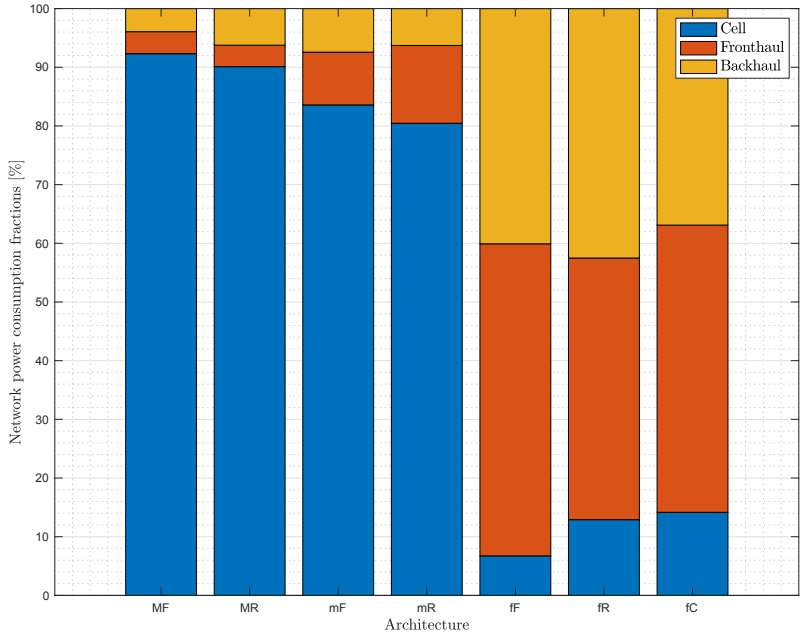

Figure 5.21: Power consumption percentages, 5G Urban Scenario.

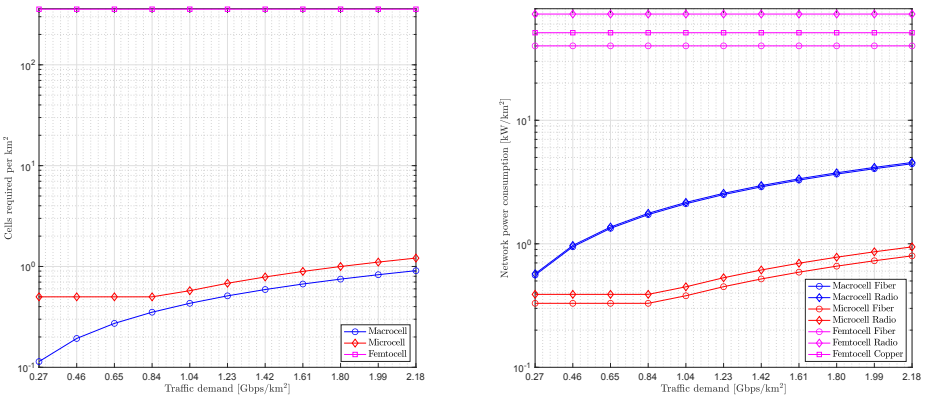

Figure 5.22: Architectures' network dimensioning and consumption, 5G Sub-urban Scenario.

Figure 5.27 shows the performance at peak data rate, where microcell represent the best options among the technologies. Gains provided by switching to optical fiber are the same as the sub-urban case. The power consumption breakdown is finally provided in Figure 5.28 and 5.29.

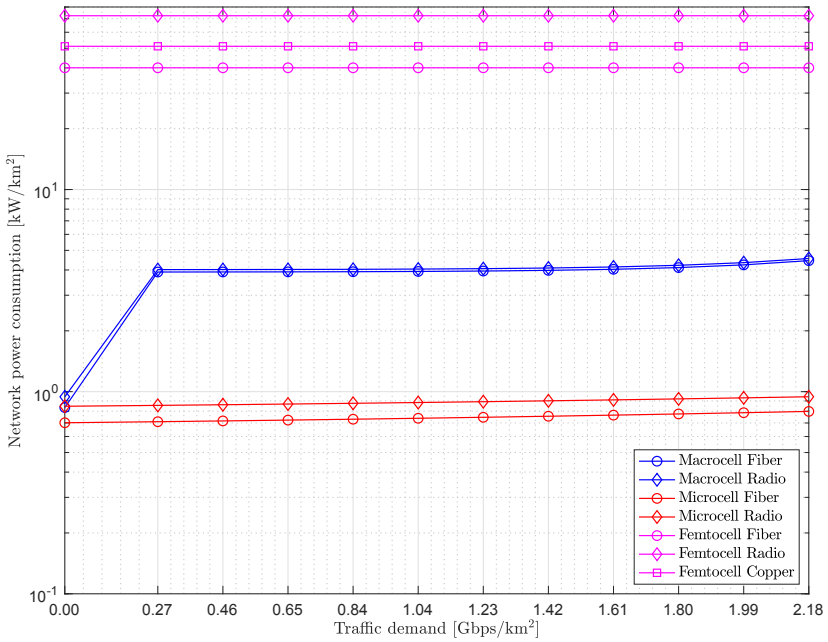

Figure 5.23: Fixed network dimensions architectures' power consumption, 5G Sub-urban Scenario.

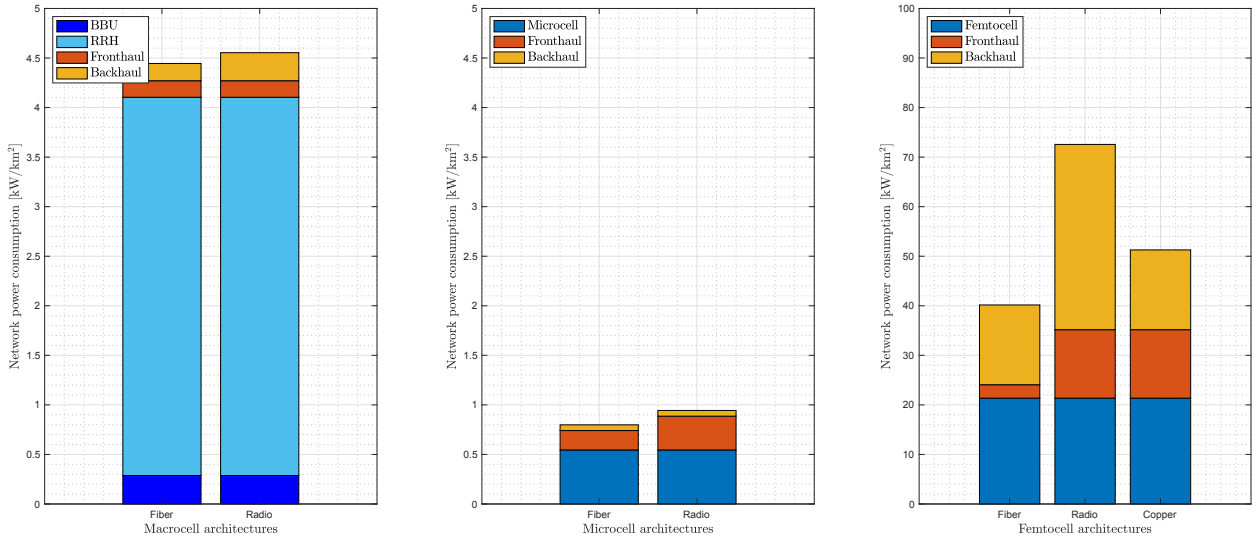

Figure 5.24: Power consumption breakdown, 5G Sub-urban Scenario.

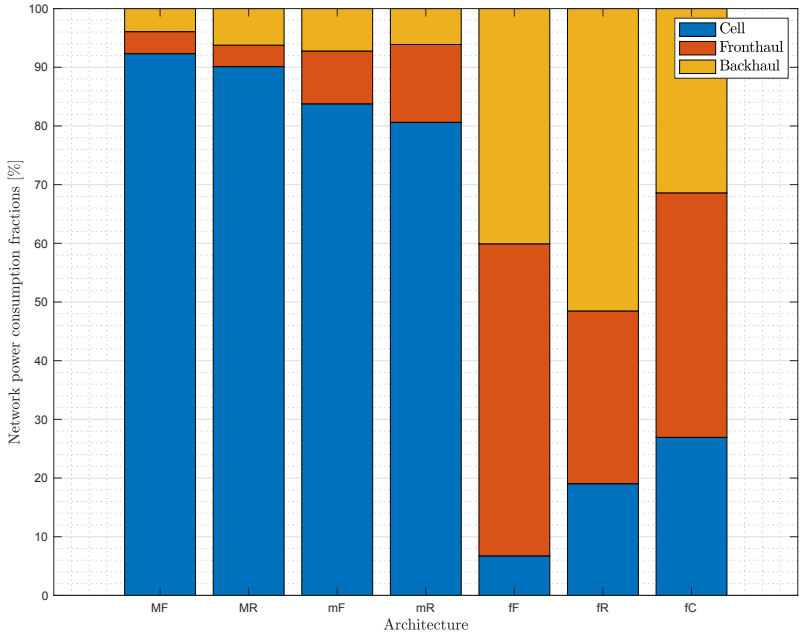

Figure 5.25: Power consumption percentages, 5G Sub-urban Scenario.

5.3 5G mmWave

In this scenario we compare mmWave StreetMacro and femtocells. Generally speaking, we find that from the power consumption perspective the same results as the non mmWave scenarios hold, with optical fiber providing the best performance among radio and copper technologies. Moreover, StreetMacro cells

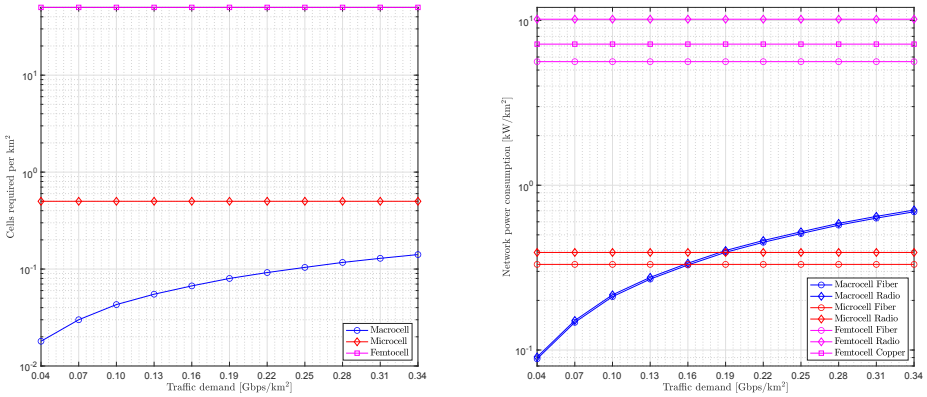

Figure 5.26: Architectures' network dimensioning and consumption, 5G Rural Scenario.

are result to be a better option than femtocells from the energy consumption perspective.

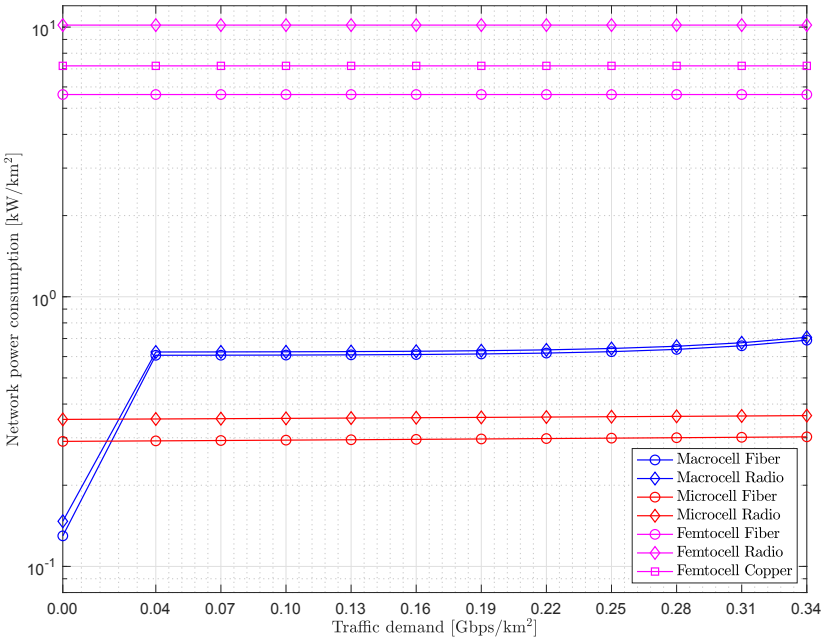

Figure 5.27: Fixed network dimensions architectures' power consumption, 5G Rural Scenario.

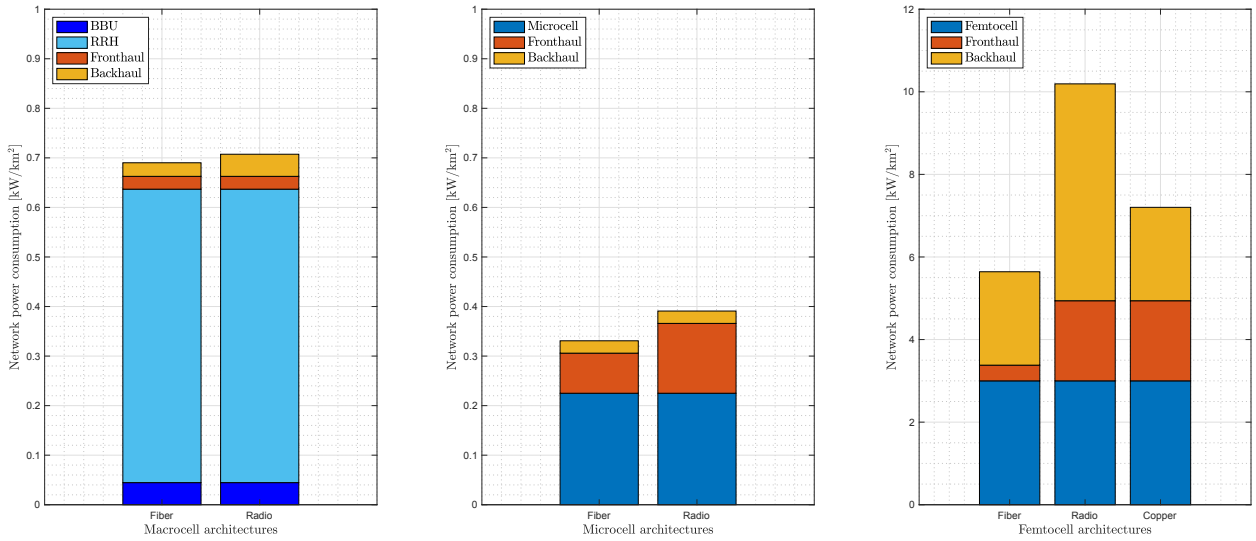

Figure 5.28: Power consumption breakdown, 5G Rural Scenario.

5.3.1 Urban Scenario

The performance in Urban scenario is reported in Figure 5.30. This illustrates the advantage in deploying StreetMacro cells: less deployments provide the necessary coverage and bandwidth demand support, while femtocells are limited by the necessity of providing spatial coverage. This leads to a trade off between the number of deployments and bandwidth demand that is won by StreetMacro cells. From the technology perspective, we observe that optical fiber provides the optimal energy performance in the scenario. Notice that only at very low levels of bandwidth demand, the spatial constraint becomes relevant, i.e., when the traffic demand goes below 1 Gbps/km^2.

Figure 5.31 shows the consumption of the cell as a function of the transmitted power, varying with the network bandwidth demand. As one can see, according to the model presented above, the variation to the overall power consumed by the cell is very tiny, and we do not observe the idle state drop down observed in the non-mmWave case depicted in the previous section.

To understand how contributions of back- and fronthaul sum up together and quantify the advantage of optical fiber, we provide the consumption breakdown in Figure 5.32. First we remark that under out hypothesis of coverage, StreetMacro cells are 100 times more energy efficient, as the number of femto to be deployed is extremely high. Secondly, we notice that the majority of the power consumption is due to the cells, which reduces the impact of a change in the technology on the overall, but still not negligible: 13% and 23% compared

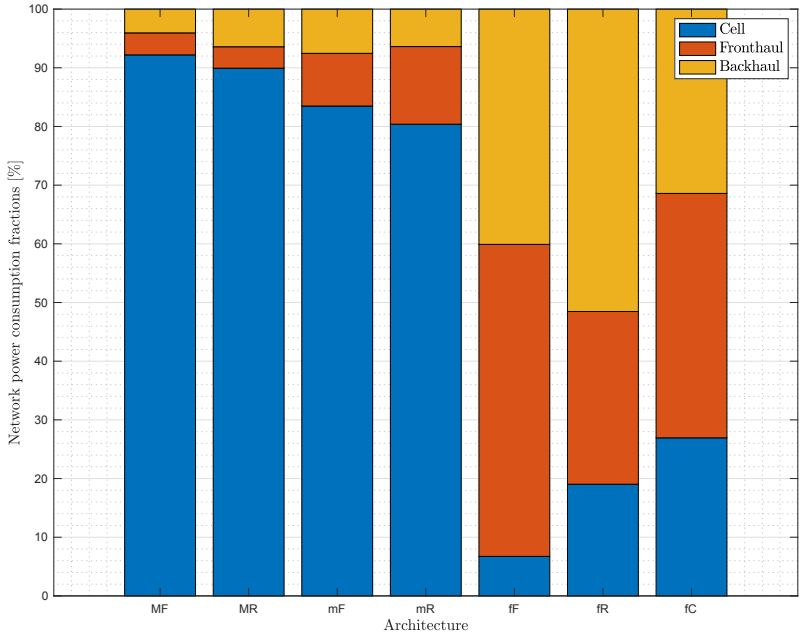

Figure 5.29: Power consumption percentages, 5G Rural Scenario.

to microwave for StreetMacro and femtocell architectures, respectively. Copper does slightly better than microwave for femtocells, but fiber is still the optimal choice. Considering only backhauling, the energy consumption reduction provided by optical fiber is more remarkable: 40% and 35% compared to radio. In femtocell scenarios, an additional gain is provided for the fronthaul part, which reduces to 30% of the counterparts when switching to optical fiber.

5.3.2 Sub-urban Scenario

The performance in Urban scenario is reported in Figures 5.33 and 5.34. All the considerations of the Urban Scenario hold for this one. Notice that in this case, due to the low amount of bandwidth predicted for this scenario, we are always in the "saturation region", i.e., where the number of cell required to provide coverage is greater than the number of cells to address the bandwidth demand.

Figures 5.35 reports the power consumption breakdown. The overall considerations as the previous case hold, however, the energy reduction provided by fiber is 13% and 54% compared to microwave in StreetMacro and femtocell scenarios, respectively. Considering backhaul only, the percentages increase to 30% and 66% for the two scenarios above, respectively. In femtocell architectures, the total energy consumption reduction for back- and fronthaul is about 77% and 50% compared to microwave and copper, respectively.

5.3.3 Rural Scenario

The performance in Urban scenario is reported in Figures 5.36 and 5.37. This scenario is very close to the Sub-urban, as the predicted bandwidth amount is not high as the Urban scenario. Despite the differences in absolute values, every conclusion and remarks as the previous case hold.

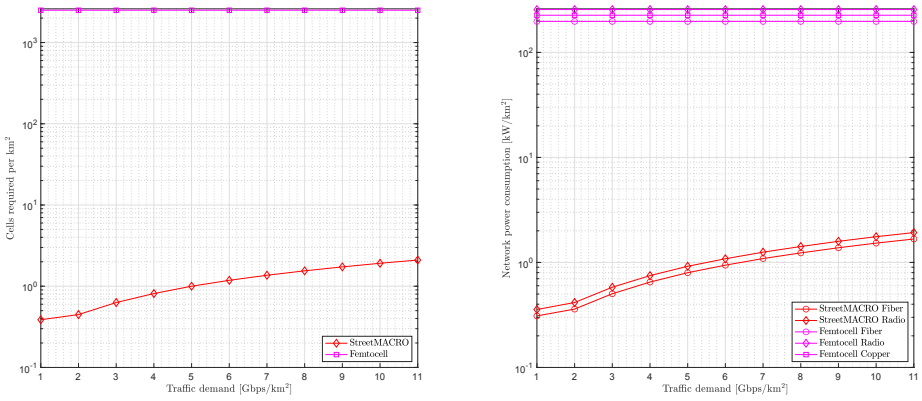

Figure 5.30: Architectures' network dimensioning and consumption, 5G mmWave Urban Scenario.

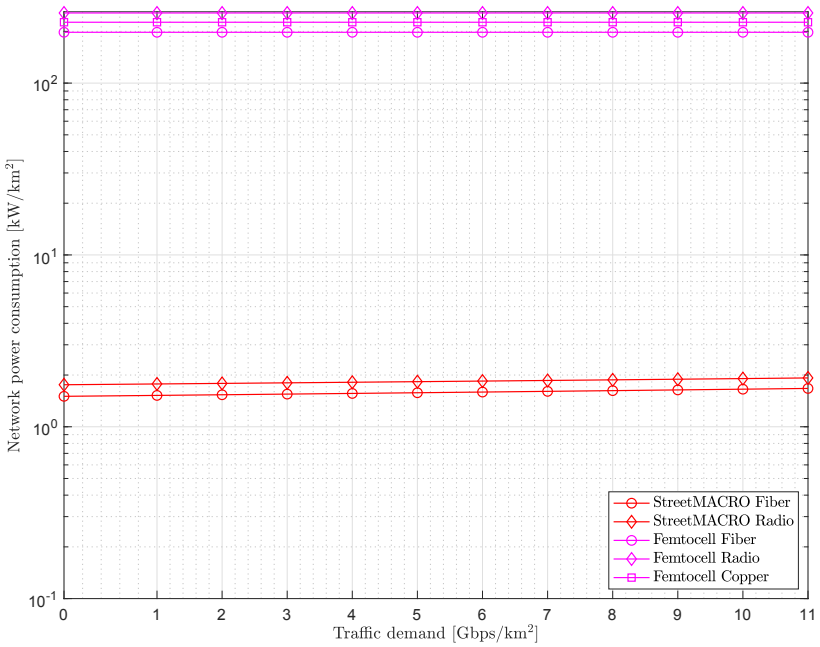

Figure 5.31: Fixed network dimensions architectures' power consumption, 5G mmWave Urban Scenario.

Figure 5.38 reports the energy consumption breakdown. The only difference with respect to the previous case relies in the percentage of energy savings of fiber versus microwave for StreetMacro, which is 14%. Other than that, the same performance and conclusions as the Sub-urban hold true.

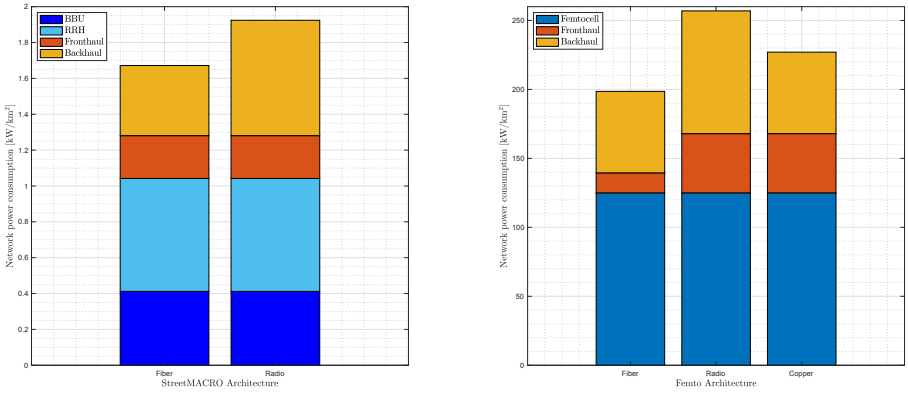

Figure 5.32: Power consumption breakdown, 5G mmWave Urban Scenario.

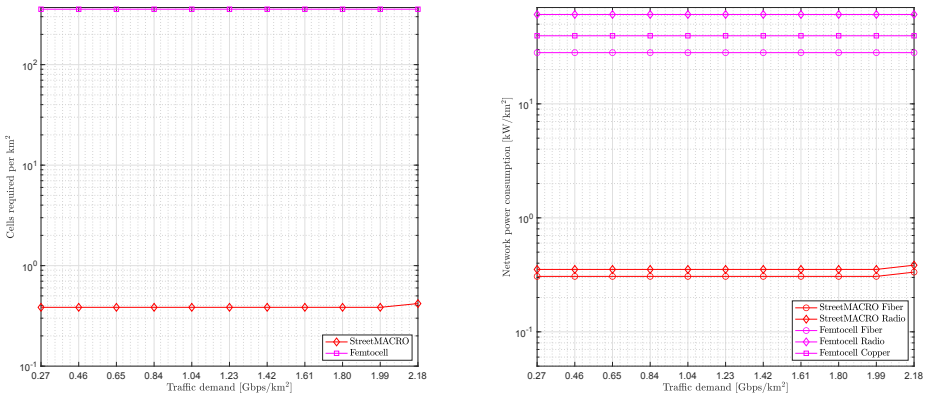

Figure 5.33: Architectures' network dimensioning and consumption, 5G mmWave Sub-urban Scenario.

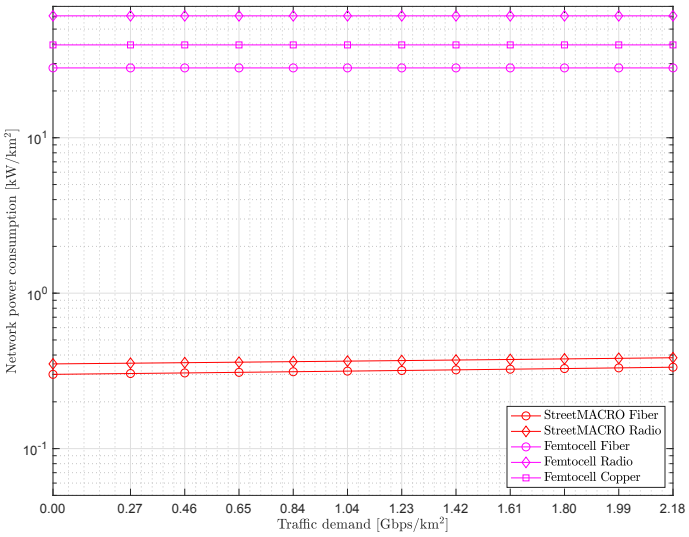

Figure 5.34: Fixed network dimensions architectures' power consumption, 5G mmWave Sub-urban Scenario.

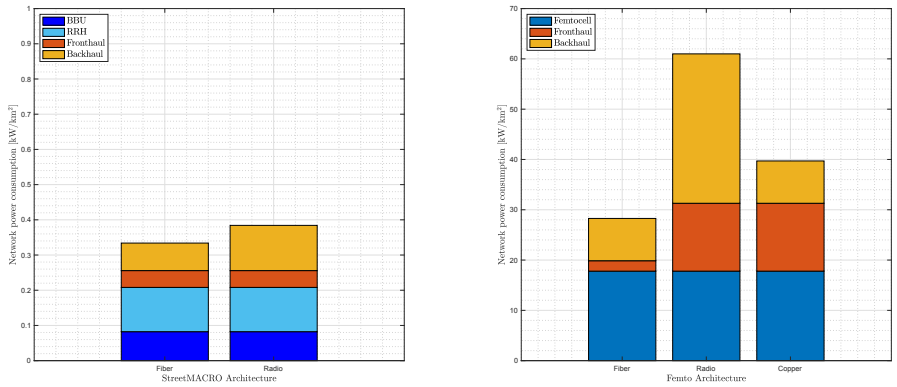

Figure 5.35: Power consumption breakdown, 5G mmWave Sub-urban Scenario.

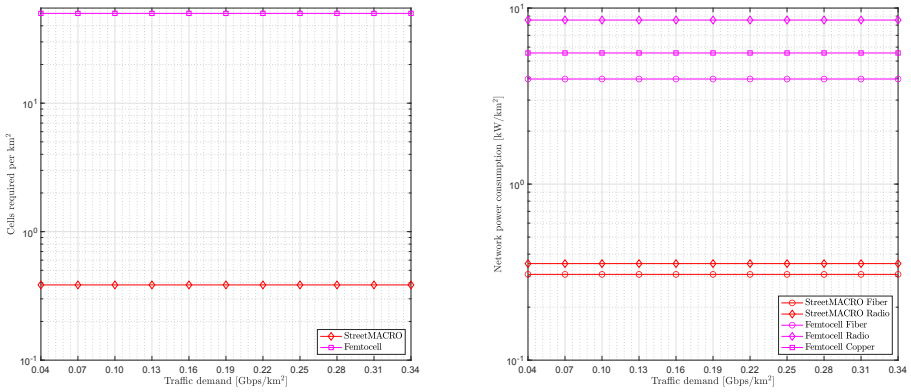

Figure 5.36: Architectures' network dimensioning and consumption, 5G mmWave Rural Scenario.

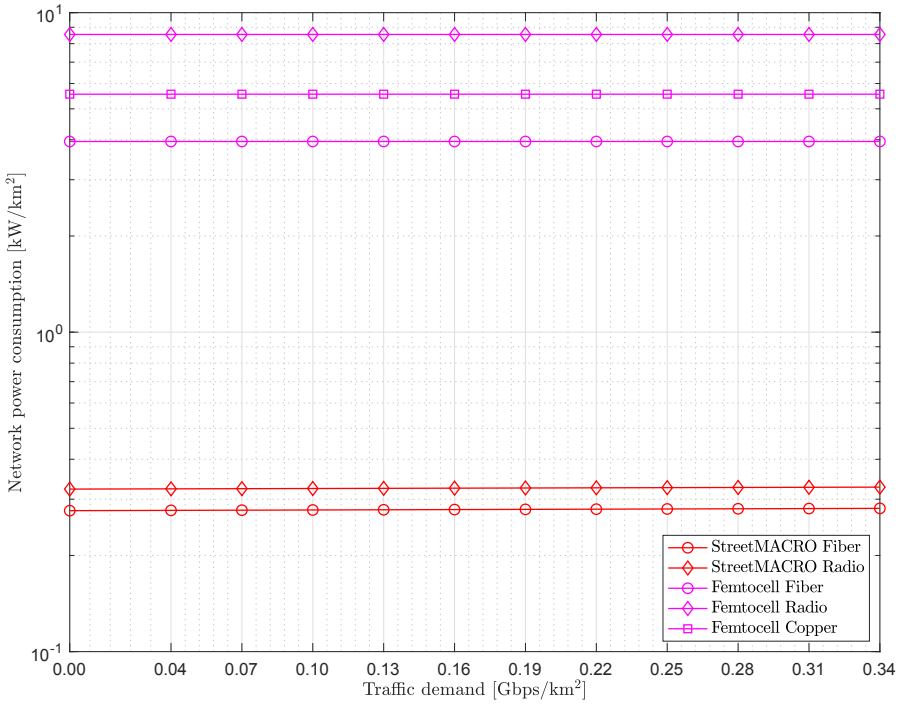

Figure 5.37: Fixed network dimensions architectures' power consumption, 5G mmWave Rural Scenario.

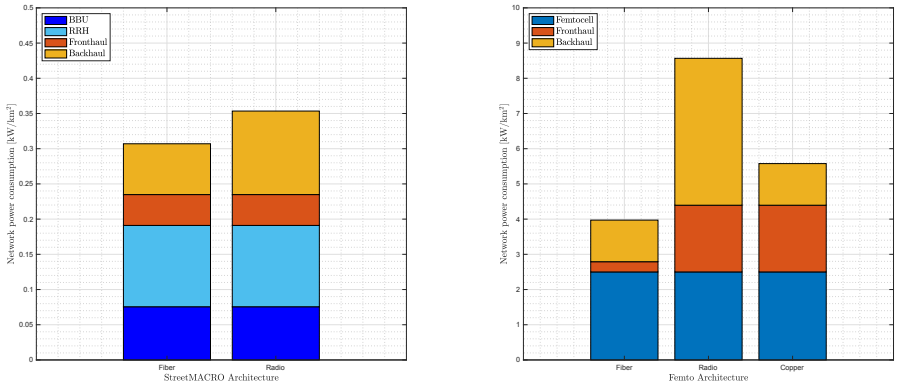

Figure 5.38: Power consumption breakdown, 5G mmWave Rural Scenario.

Chapter 6

Conclusions

In this study we addressed the problem of finding which front- and backhauling technology among optical fiber, radio link, copper, satellite and FSO provides the best performance in terms of energy consumption in conventional 4G and 5G scenarios. We selected the main scenarios envisioned by 3GPP and ETSI and explored the literature work on the subject, which mostly claims optical fiber to be the most convenient technology for front- and backhaul infrastructures [2, 3, 40–42]. We collected data from independent sources and built a database to run an energy consumption model tailored to the selected scenarios, including data from the literature, brochures/data sheets and telcos.

Considering 4G technology, the results obtained by the model, resumed in Table 6.1, show that optical fiber provides the best performances in terms of energy consumption in all the considered scenarios, with gains between 21% to 54% compared to microwave technology in macro- and microcell scenarios, while peaking to 79% compared to radio in femtocell scenarios. Isolating the power consumption contributions, backhaul is the most energy demanding between cells and fronthaul. Adopting optical fiber allows for power savings from 54% to 94% on the backhaul deployment.

Considering 5G technology, optical fiber is still the optimal solution in terms of energy consumption savings, with overall reduction of 2% to 15% in macro- and microcells, as reported in Table 6.2. When considering femtocells, power consumption results to be tens of times higher. and optical fiber allows for a reduction in the ranges of 8% to 45% compared to copper and microwave solutions. As for 4G backhaul provides the highest energy consumption.

The same considerations apply also for 5G mmWave technology, whose results are summed up in Table 6.3

Additionally, the results show that over-dimensioning a network is not an optimal approach: even if a network works in idle state, it will be using more power than a smaller network working with an higher traffic load.

	vs Radio-Link	vs Radio-Link	vs Radio-Link	vs Copper
Architecture & Scenario	MACROCELLS	MICROCELLS	FEMTOCELLS	FEMTOCELLS
Urban	21	39	36	32
Suburban	21	39	62	54
Rural	20	39	63	54

Table 6.1: Power savings of fiber in 4G technology [%]

	vs Radio-Link	vs Radio-Link	vs Radio-Link	vs Copper
Architecture & Scenario	MACROCELLS	MICROCELLS	FEMTOCELLS	FEMTOCELLS
Urban	2	15	16	8
Suburban	2	16	45	22
Rural	2	15	45	22

Table 6.2: Power savings of fiber in 5G technology [%]

	Fiber over Radio-Link	Fiber over Radio-Link	Fiber over Copper
Architecture & Scenario	MACROCELLS	MICROCELLS	FEMTOCELLS
Urban	13	23	13
Suburban	13	54	29
Rural	14	54	29

Table 6.3: Power savings of fiber in 5G mmWave technology [%]

Bibliography

[1] "5g power: Creating a green grid that slashes costs, emissions & energy use." https://www.huawei.com/en/technology-insights/publications/huawei-tech/89/5g-power-green-grid-slashes-costs-emissions-energy-use, 2020.

[2] F. Farias, M. Fiorani, S. Tombaz, M. Mahloo, L. Wosinska, J. Costa, and P. Monti, "Cost- and energy-efficient backhaul options for heterogeneous mobile network deployments," *Photonic Network Communications*, vol. 32, 12 2016.

[3] M. Mahloo, P. Monti, J. Chen, and L. Wosinska, "Cost modeling of backhaul for mobile networks," in *2014 IEEE International Conference on Communications Workshops (ICC)*, pp. 397–402, 2014.

[4] "Packetlight networks optical devices power consumption." https://www.packetlight.com/products/1g-to-40g-services/, 2021.

[5] "Sino-telecom optical devices power consumption." http://www.sino-telecom.com/Product/list.aspx?lcid=10, 2021.

[6] "PTP 850E Microwave Radio." https://www.cambiumnetworks.com/wp-content/uploads/2021/03/Cambium_Networks_data_sheet_PTP_850E.pdf.

[7] M. Araújo, L. Ekenberg, and J. Confraria, "Satellite backhaul for macrocells, as an alternative to optical fibre, to close the digital divide," in *2019 IEEE Wireless Communications and Networking Conference (WCNC)*, pp. 1–6, 2019.

[8] S. Bolis, D. Scazzoli, L. Reggiani, M. Magarini, and M. M. Alam, "A study on beamforming for coverage of emergency areas from uavs," in *2019 UK/China Emerging Technologies (UCET)*, pp. 1–4, 2019.

[9] F. Alagoz and G. Gur, "Energy efficiency and satellite networking: A holistic overview," *Proceedings of the IEEE*, vol. 99, no. 11, pp. 1954–1979, 2011.

[10] M. Martinelli and P. Martelli, *Fundamentals of Optical Communications*. Wiley Series in Microwave and Optical Engineering, Wiley, 2026.

[11] "Hybrid free-space optics/radio frequency (fso/rf) links for fronthaul network within 5G paradigm." `https://atc.mise.gov.it/images/documenti/Rivista/2017-2018/05_collegamenti_fso.pdf`, 2018.

[12] A. Douik, H. Dahrouj, T. Y. Al-Naffouri, and M.-S. Alouini, "Hybrid radio/free-space optical design for next generation backhaul systems," *IEEE Transactions on Communications*, vol. 64, no. 6, pp. 2563–2577, 2016.

[13] H. Refai, J. Sluss, H. Refai, and M. Atiquzzaman, "Comparative study of the performance of analog fiber optic links versus free-space optical links," *Optical Engineering - OPT ENG*, vol. 45, 02 2006.

[14] 3GPP TR 38.913 V14.3.0, "5G; study on scenarios and requirements for next generation access technologies," tech. rep., 3GPP, 2018.

[15] N. Carapellese, A. Pizzinat, M. Tornatore, P. Chanclou, and S. Gosselin, "An energy consumption comparison of different mobile backhaul and fronthaul optical access architectures," in *2014 The European Conference on Optical Communication (ECOC)*, pp. 1–3, 2014.

[16] G. Auer, V. Giannini, I. Godor, P. Skillermark, M. Olsson, M. A. Imran, D. Sabella, M. J. Gonzalez, C. Desset, and O. Blume, "Cellular energy efficiency evaluation framework," in *2011 IEEE 73rd Vehicular Technology Conference (VTC Spring)*, pp. 1–6, 2011.

[17] R. Bassoli, F. Granelli, S. T. Arzo, and M. Di Renzo, "Toward 5g cloud radio access network: An energy and latency perspective," *Transactions on Emerging Telecommunications Technologies*, vol. 32, no. 1, p. e3669, 2021. e3669 ett.3669.

[18] M. Deruyck, W. Joseph, and L. Martens, "Power consumption model for macrocell and microcell base stations," *Transactions on Emerging Telecommunications Technologies*, vol. 25, 03 2014.

[19] H. Holma, A. Toskala, and T. Nakamura, *5G Technology: 3GPP New Radio*. Wiley, 2020.

[20] M. Fiorani, S. Tombaz, J. Martensson, B. Skubic, L. Wosinska, and P. Monti, "Modeling energy performance of c-ran with optical transport in 5g network scenarios," *Journal of Optical Communications and Networking*, vol. 8, no. 11, pp. B21–B34, 2016.

[21] L. Nan, "The next journey for 5G." Presentation.

[22] M. Deruyck, D. Vulder, W. Joseph, and L. Martens, "Modelling the power consumption in femtocell networks," *IEEE Wireless Communications Networking Conference (WCNC), Paris, France*, 04 2012.

[23] J. C. Mayeda, D. Lie, and J. Lopez, "A high efficiency fully-monolithic 2-stage c-band gan power amplifier for 5G microcell applications," in *2018 Texas Symposium on Wireless and Microwave Circuits and Systems (WMCS)*, pp. 1–4, 2018.

[24] "5G power consumption: How mmwave and c-band compare." https://frankrayal.com/2021/03/15/how-mmwave-and-c-band-compare-on-power-consumption/.

[25] ITU-T, "Sustainable power-feeding solutions for 5G networks," tech. rep., ITU, 2019.

[26] "5G In-building High Power RU." https://hfrnet.com/front/product/productDetail/134.

[27] "5g in-building low power ru." https://hfrnet12.gabia.io/front/product/productDetail/133.

[28] "Streetmacro 6701 spec sheet." https://it.scribd.com/document/494070964/Streetmacro-6701-Spec-sheet.

[29] "Baseband 6648 description." blob:https://pdfcoffee.com/adac2b72-c059-499d-8f92-cc299dbcdc32.

[30] "How 5G is bringing an energy efficiency revolution." https://onestore.nokia.com/asset/f/207360.

[31] "Router 6673." https://www.ericsson.com/4a4ba6/assets/global/eridoc/405880/09004cffc855642c.pdf.

[32] "5G Open vRAN - vDU vCU." https://hfrnet.com/front/product/productDetail/147.

[33] "VRAN 2.0 ON HPE INFRASTRUCTURE." https://h50146.www5.hpe.com/products/servers/document/pdf/edgeline/vran2.0.pdf.

[34] "5g sa vcore." https://hfrnet.com/front/product/productDetail/146.

[35] "HPE ProLiant DL380 Gen10 Server - Specifications." https://support.hpe.com/hpesc/public/docDisplay?docId=a00019683en_us&docLocale=en_US.

[36] E. J. Oughton, Z. Frias, S. van der Gaast, and R. van der Berg, "Assessing the capacity, coverage and cost of 5g infrastructure strategies: Analysis of the netherlands," *Telematics and Informatics*, vol. 37, pp. 50–69, 2019.

[37] X. Liu, *Optical Communications in the 5G Era*. Academic Press, Oct 2021. Google-Books-ID: QYEqEAAAQBAJ.

[38] "5G Power: Creating a green grid that slashes costs, emissions & energy use." https://www.huawei.com/en/technology-insights/publications/huawei-tech/89/5g-power-green-grid-slashes-costs-emissions-energy-use.

[39] "Fattore di emissione di co2 e consumo di energia primaria per kilowattora di energia elettrica al contatore." http://kilowattene.enea.it/KiloWattene-CO2-energia-primaria.html.

[40] J. Baliga, R. Ayre, K. Hinton, and R. S. Tucker, "Energy consumption in wired and wireless access networks," *IEEE Communications Magazine*, vol. 49, no. 6, pp. 70–77, 2011.

[41] P. Monti, S. Tombaz, L. Wosinska, and J. Zander, "Mobile backhaul in heterogeneous network deployments: Technology options and power consumption," in *2012 14th International Conference on Transparent Optical Networks (ICTON)*, pp. 1–7, 2012.

[42] S. Tombaz, P. Monti, K. Wang, A. Vastberg, M. Forzati, and J. Zander, "Impact of backhauling power consumption on the deployment of heterogeneous mobile networks," in *2011 IEEE Global Telecommunications Conference - GLOBECOM 2011*, pp. 1–5, 2011.